TABLE OF CONTENTS

List of Figures

LIST OF TABLES

Chapter 1
1 Introduction

The wireless industry has grown at a tremendous pace in the past two decades. In the 1980's, the word 'wireless' was synonymous with a cellular phone or a cordless phone. However, today the focus of the wireless industry has shifted from wireless voice service to wireless data service. Wireless LANs have become popular and the demand continues to grow. Wireless data services are being offered on cell phones and Personal Digital Assistants (PDAs). Research is underway in bringing multi-media content to the wireless subscriber. All this new content will require a much higher data rate when compared to the wireless systems used currently. The data rates for the second-generation systems that are often used today are on the order of a few kilobits per second. The third generation of wireless systems popularly known as "3G" is currently under development and promises to deliver data up to 2 Mbits/second to the wireless end user [1]. The advances in the fields of smart antennas, signal processing and hardware design have all helped to increase the effective data rate available to the end user.

The advantages due to these developments will require the wireless system to be well-planned and deployed efficiently. The wireless channel inherently limits the performance of the wireless system. Unlike a wired system, the physical objects and the environment that surrounds the system play an important role in the performance of the wireless system. The design of the wireless system will require careful planning and prediction of the coverage and interference levels [2].

Statistical and empirical techniques have traditionally been used to predict the coverage of a wireless system. Most of the statistical techniques use simple path loss exponent models for large-scale path loss estimation [3]. The path loss exponent was calculated based on the measurements conducted in the environment where the wireless system is deployed. Only a crude estimate of the average path loss can be obtained using this method. Moreover, the extensive measurements are prohibitively expensive, especially for high data rate applications. These models can only be used to estimate the path loss or the mean signal strength. The wide band characteristics of the channel such

as the power delay profile or the delay spread cannot be estimated using these techniques. However, it has been proven that the shape of the power delay profile and the delay spread can significantly affect the performance of a mobile communication system [4].

In the 1990's, a host of new propagation models which used site-specific information to predict the propagation characteristics were introduced; an approach based on ray tracing being the most prominent among them. A ray tracing-based approach can be used to predict the small area average receiver power, and wide band characteristics of the channel such as the root-mean square delay spread, the angle of arrival and the slow fading correlation of the different environments [5]. However, unlike the traditional statistical models, which need very little or no information regarding the environment, a ray tracing technique must accurately model all the physical objects in the environment. There has been very little research in the area of modeling of physical objects for propagation prediction. The first part of this thesis implements a method to model the buildings and the terrain using the geographic data available from commercial sources.

Chapter 2 describes the different geographic data products that are currently available, which could help us in modeling the environment. The issues related to the modeling of the terrain are discussed in Chapter 3. The different algorithms that can be used to model the terrain are implemented and are compared with one another. Chapter 4 describes a method to model the buildings and to combine the building information with the terrain data.

The latter part of the thesis discusses different ray tracing techniques used to predict the propagation characteristics of the wireless system. Chapter 5 presents an overview of the different ray tracing techniques that can be used to predict the propagation characteristics of the channel. For designing a wireless point to multi-point network such as a Wireless LAN or a cellular system, the propagation characteristics of multiple points in space need to be estimated. The ray tracing based prediction algorithms are notorious for their computational complexity, especially when the propagation characteristics of multiple receivers need to be estimated. A novel, computationally less intensive prediction technique for predicting the signal characteristics of multiple

receivers is introduced in Chapter 6. This technique is compared with the standard ray tracing technique in terms of its computational speed and accuracy.

Appendix A provides a reference for the programs used to model the terrain and the buildings. Appendix B describes the free space propagation model used for ray tracing applications.

The work pertaining to the first few chapters of this thesis was done while the author served as a Graduate Summer Intern with Wireless Valley Communications, Inc. The work pertaining on the rest of the thesis was performed while working as a Graduate Research Assistant with the Mobile Portable Radio Group in Virginia Tech. This thesis was sponsored in part by the National Science Foundation as a part of its research project named “A Collaborative Problem-Solving Environment for Modeling of Broadband Wireless Communication Systems”.

Chapter 2
2 Geographic data for Site-specific propagation prediction

This chapter provides an overview on the different commercial products available that can be used to model the environment for site-specific propagation prediction. The chapter also discusses about the data format most suitable for modeling the environment.

2.1 Introduction

A ray tracing based prediction technique would require a very detailed description of the physical environment. Some of the earlier ray optics based propagation prediction models used Digital Terrain Models (DTMs) with the building heights superimposed on them to do propagation prediction [6]. The DTMs are raster databases where the elevations of a regularly spaced grid of points are stored. The raster database limits the applicability of the ray tracing software. The problems of using a raster database for a ray tracing based application is discussed in the next section. Some other ray optical models use 2-D database of the cities, which are easily available from city maps [7] or use the street and the terrain data for modeling propagation [8].

Until recently, the limited availability of high-resolution geographic data was the stumbling block in modeling the environment. With the new advances in the field of remote sensing and image processing, high-resolution databases of the different cities throughout the United States are now available. This chapter focuses primarily on the geographic products available that can be used for modeling the environment for a site-specific propagation prediction technique based on ray tracing.

The first part of the chapter discusses about the data format that is most suitable for modeling the environment and the desirable characteristics of the environment database. The latter half of the chapter gives a survey of the different products available in the market, which can be used to model the environment.

2.2 Data Format for Modeling the Environment

There are two fundamentally different ways of representing an image in a digital computer; the raster and the vector format.

In the raster format, every point in the specified space is identified with a value. A typical example of a raster database is a bitmap image, where the color of every point or pixel of the image is given. In the case of a raster format for a 3-D model, the elevation of the different points may be specified. For example a terrain might be represented as a rectangular grid where the elevation of the grids are given. A raster image of the terrain or of any physical environment can be obtained from the satellite images or from other aerial photographic techniques. Note that the raster image of a physical environment need not just contain the elevation of the points; it might also have information about the soil characteristics, the population density or any other parameter. Most of the images used in the every day world such as BitMap formats (.BMP), JPEG formats (.JPEG) and JPG formats (.JPG) are in the raster format.

The term vector format is used here to mean the representation for a point in some logical space. In dealing with three-dimensional (3-D) vector systems, three spatial coordinate axes X, Y and Z are typically used to represent a point in space. The vector database specifies the boundaries of the vector space used. In other words, to represent lines, circles or other compound shapes, a vector database uses a sequence of points. For instance a line in 3-D space is usually specified with a starting point and an end point. Polygons are typically specified as a set of 3-D vector points, which correspond to the vertices of the polygons. Many CAD software tools like AutoCAD uses vector formatted images while representing an image. The vector format is usually more economic in storage when compared to raster image formats.

The raster data generally occupies a larger storage area when compared to a vector database. Moreover, the raster data is not flexible enough to represent all the details of an object completely. For example, a raster data representation of the building cannot include the surfaces, which are inside the building and it would be unable to

model an indoor-outdoor propagation model using ray tracing techniques. Hence most of the ray tracing implementations prefer a vector database.

2.3 Desirable Characteristics of an Environment Database

The most convenient environment database for a 3-D ray tracing software consists of many flat planar polygons that represent the surfaces of buildings and terrain. A large proportion of surfaces that cause any significant effect on the propagation of radio waves, such as walls, roofs, and partitions. can be modeled as flat polygons. Flat polygons are easy to describe numerically and allow simple reflection calculations. The flat polygons have clear edges and corners, which makes it easier to model diffraction. A polygon based environment model can be constructed easily using CAD tools. Hence a vector model of the terrain with flat polygons is most suited for 3-D ray tracing.

The description of the environment has to be complete and as error free as possible to obtain accurate results for the predictions. This would mean that a large number of surfaces would have to be modeled while describing the environment. However, the computational complexity of a ray tracing software increases with the total number of surface [9]. Therefore, a balance between these two requirements has to be achieved.

2.4 Geographic Data Sources

An indoor database can be modeled using the architectural plan for the buildings. In some cases, in which CAD tools like AutoCAD are used for designing the building, the building database is readily available in a vector format.

A database, which describes the outdoor environment, should include the details of all the buildings and the terrain in that region. Remote sensing methods are employed to obtain the geographic information of a particular region. One of the earliest and the most popular remote sensing methods is aerial photography. As technology progressed, the remote sensing expanded from aerial photography to encompass imagery of the land surface collected by electronic sensors sensitive to a wider range of electromagnetic

energy as well as sonar energy [10]. With the advances in the field of remote sensing and image analysis, high-resolution data, which describes both the terrain and the buildings of a particular region, is now available.

The United States Geological Survey (USGS) produces high resolution mapping data for land use and terrain elevation, line graphics of major cartographic features and high resolution photographic data [11]. Currently the terrain maps of almost all of the territories of the USA can be obtained from USGS. Apart from the USGS, there are many private vendors like I-Cubed Inc [12] and EDX Corporation [13] that provide information regarding the terrain, buildings and morphology data for many cities across the United States. Today, there exists specialized Geographic Information System packages like ArcInfo that helps the user to manage, display, query, and analyze geographical data obtained from any source. The next section surveys a host of products available in the market that can be used for modeling an outdoor environment.

2.4.1 Digital Ortho-image

Digital Ortho-image denotes an image of a city or an area obtained from either air photos or satellite imagery. This information is often used as a visual reference of the area under consideration.

Figure 2.1: Ortho Imagery of Old Town, Ft Collins CO.
(Source: Wireless Valley Communication, Inc. in conjunction with I-Cubed)

2.4.2 USGS DEMs

The most popular product from the USGS is called a 'DEM' or a Digital Elevation Model. The USGS DEMs consists of an array of elevations for ground positions at regularly spaced intervals. The data is produces either from digitized cartographic map contour overlays or from scanned National Aerial Photography Program (NAPP) photographs. USGS DEMs are generally available in resolutions of 30 meters. The vertical resolution is often equal to 15 meters. The 30-meter data typically provides the elevation of a 2 dimensional array of data spaced 7.5 arc-minutes apart in latitude and longitude and hence it is popularly known as 7.5 minute DEM. The USGS DEMs are usually used to represent the terrain characteristics of a particular region.

However, DEMs with a resolution as low as 30 meters fails to capture all the building details and other man made or natural obstacles that might be required to plan a wireless network in an urban environment. Currently DEMs with a resolution as fine as 10 meters are available for select regions. Fig. 2.2 shows a gray scale image of a DEM with 10m x 10m resolution of the Lake Tahoe region in CA [14]. The pixels with a higher gray scale value (brighter) denote higher elevations and the pixels with lower gray scale values (darker) denote lower altitudes.

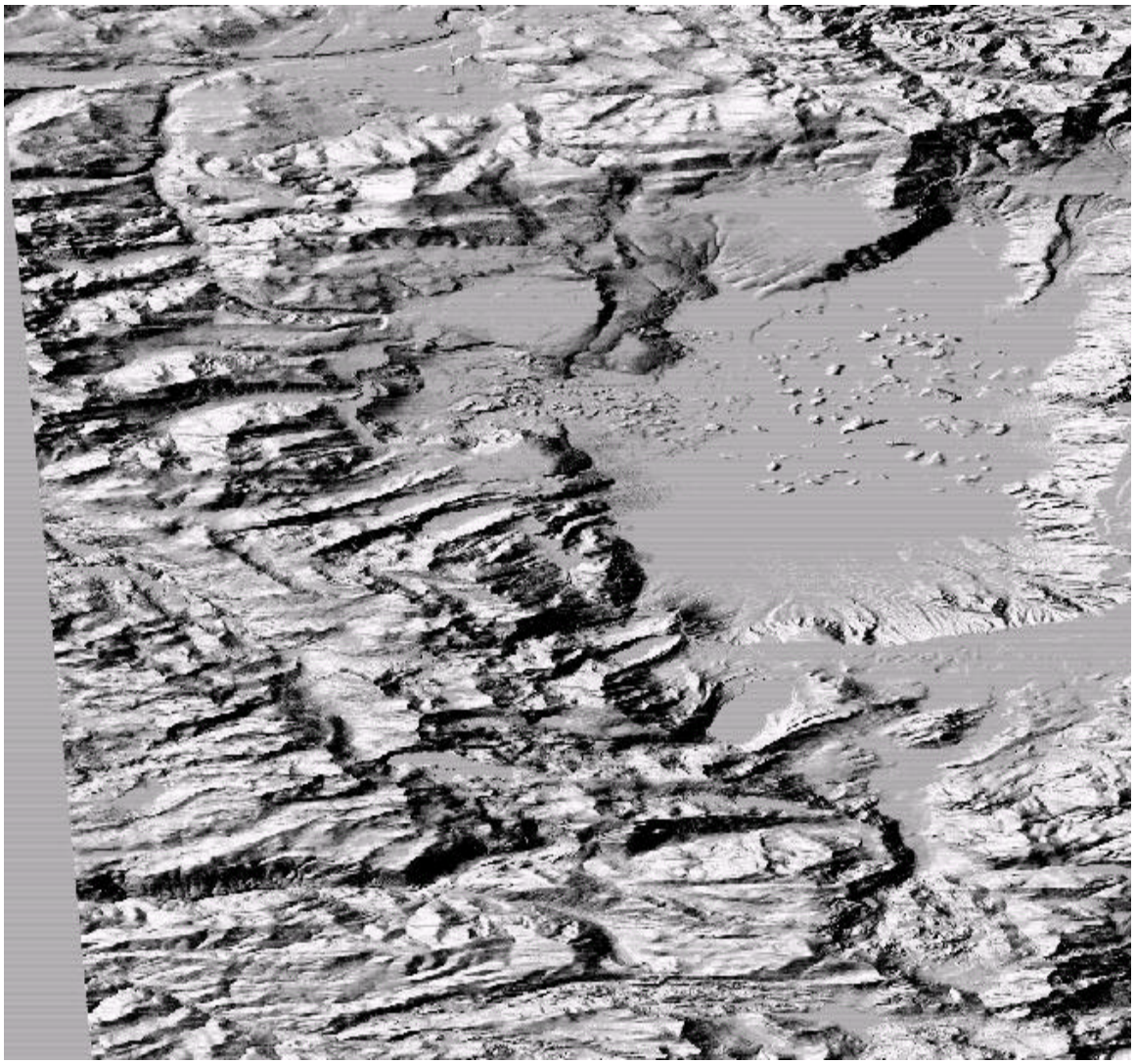

Figure 2.2: A 7.5 minute DEM of the Lake Tahoe Area in California (Source: http://blt.wr.usgs.gov/tahoe/IMG/dem_image_s.jpg)

2.4.3 Land Use and Land Cover Digital Data (LULC)

LULC is a product of the USGS that is derived from thematic overlays registered to 1:250,000-scale base maps and a limited number of 1:100,000-scale base maps. LULC data provide information on urban or built-up land, agricultural land, rangeland, forestland, water, wetlands, barren land, tundra, and perennial snow or ice. Associated

maps display information in five data categories: (1) political units, (2) hydrologic units, (3) census county subdivisions, (4) federal land ownership, and (5) state land ownership.

2.4.4 Canopy DEM

A Canopy DEM represents the elevation of a grid of a surface that can be visualized as if a thin blanket was draped over a city. A Canopy DEM consists of an array of elevations at regularly spaced intervals and hence has a raster data format. It includes surface height data for trees and buildings and the terrain. Canopy DEMs are developed from stereo aerial photographs using automated photogrammetric techniques. Digital elevation models works very well in areas where buildings are less than 15m tall (residential). Now high-resolution canopy DEMs with resolution as fine as 1m x 1m are available for many cities throughout the United States. The height resolution available is also 1 meter. The details of the buildings and other obstacles can be extracted from a Canopy DEM with a resolution of 1m x 1m x 1m. A canopy DEM is stored in the raster format. Canopy DEM's can be used to model the terrain and the buildings for a ray tracing based prediction technique where an accurate model of the physical environment is required. Fig. 2.3 shows a cross section of a Canopy DEM of downtown Chicago. The resolution of this DEM is 1m x 1m x 1m. Canopy DEMs of the different cities across the USA, are available from many private vendors such as I-Cubed Inc and EDX Corporation.

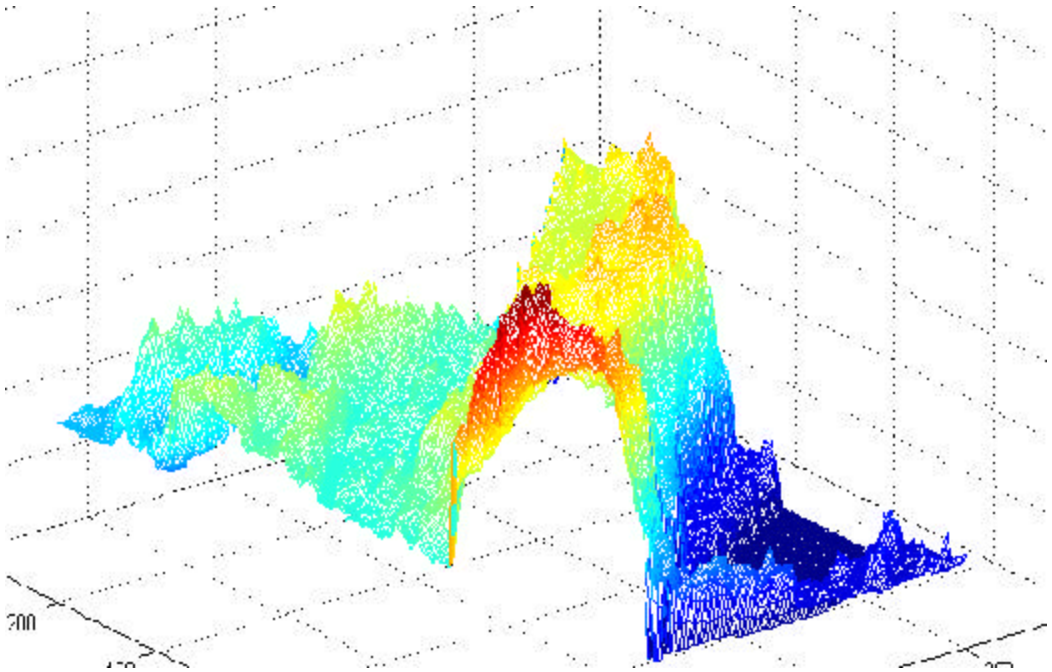

Figure 2.3: A cross section of a canopy DEM of downtown Chicago (Source: Wireless Valley Communications, Inc. in conjunction with I-Cubed) The 2-D rater data is visualized using Matlab.

2.4.5 Bald Earth DEM

A Bald Earth DEM can be visualized as the elevation of the earth with all trees and buildings removed. Bald Earth DEM is developed from canopy DEMs and ground survey data. The low points from the Canopy DEM (usually streets) are captured and interpolated to find the elevation of the terrain. Bald Earth DEM is used as a reference to define the height of buildings relative to the local ground surface. Bald Earth DEMs with a resolution of 1m x 1m x 1m are currently available from various sources such as I-Cubed Inc. and Geo Strategy Inc. (Fig. 2.4)

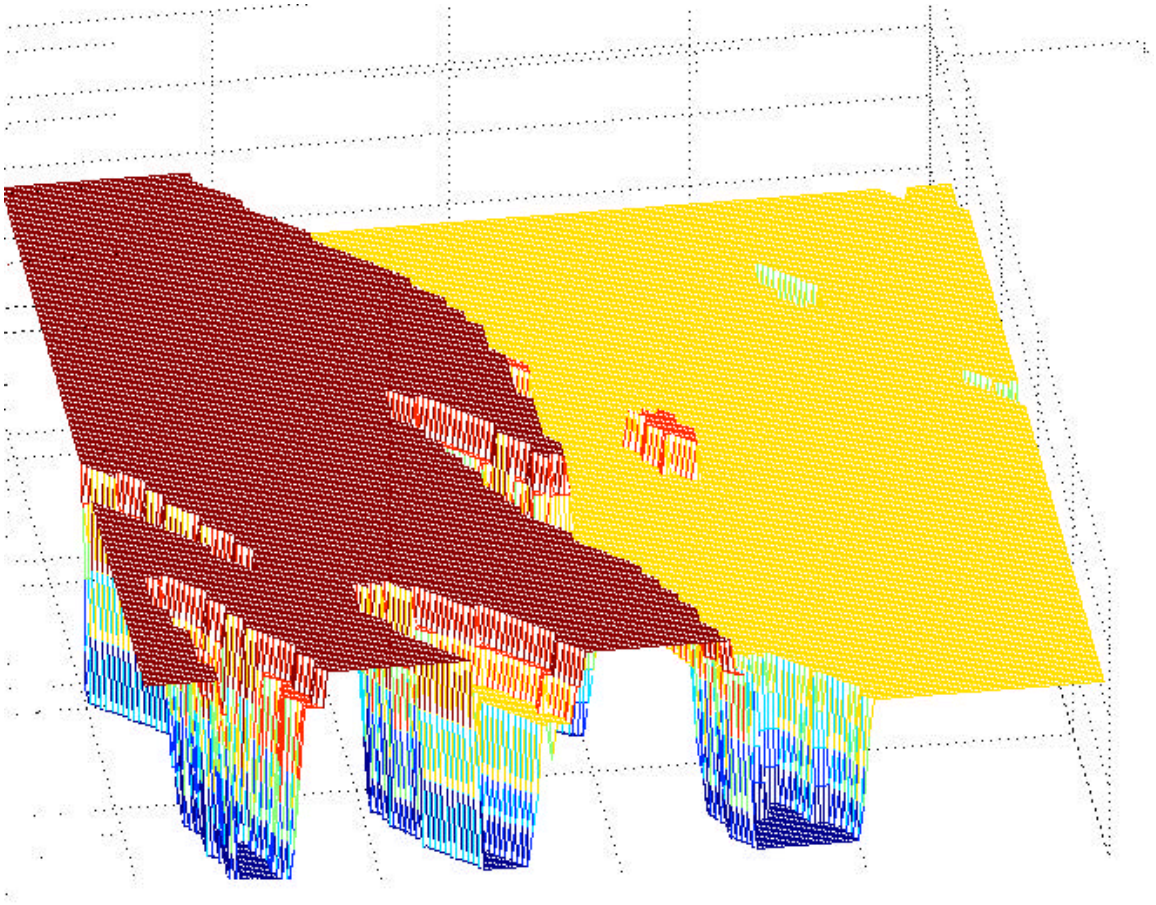

Figure 2.4: The Bald Earth DEM of downtown Chicago.
(Source: Wireless Valley Communications, Inc. in conjunction with I-Cubed).
The 2-D rater data is visualized using Matlab.

2.4.6 Building Foot-Prints

The Building Foot-print is a vector representation of the foot-prints of the exterior walls of the buildings. The footprints of exterior walls of the buildings are represented as a polygon and the coordinates of the vertices of the polygons are stored. This information is developed from ground survey measurements and the Canopy DEM. The building foot-print information is used while modeling the buildings for propagation prediction. Chapter 4 explains the process of modeling the buildings. This product is also available from private vendors such as I-Cubed Inc. and GeoStrategy Inc.

2.4.7 Flooded Engineering DEM

Flooded Engineering DEM integrates the fine detail of the Building heights with the broad area coverage of the Bald Earth DEM. The elevations of the buildings are added to the terrain elevation of the Bald Earth DEM to obtain the Flooded Engineering DEM. The elevations of the buildings are obtained by using the building foot print information and the Canopy DEM. The flooded Engineering DEMs do not include many other obstacles such as vegetation growth. Flooded Engineering DEM with a resolution of 1m x 1m x 1m is currently available (Fig. 2.5).

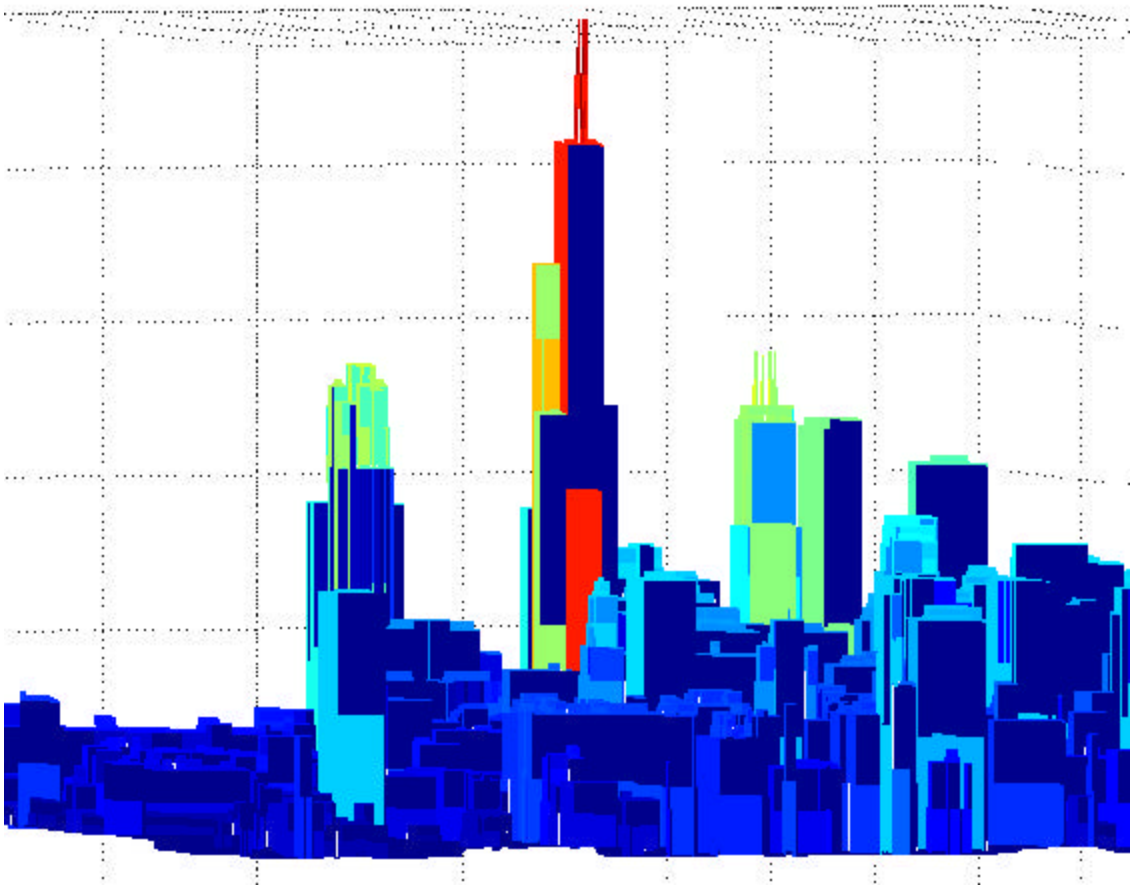

Figure 2.5: Flooded Engineering DEM of downtown Chicago.
(Source: Wireless Valley Communications, Inc. in conjunction with I-Cubed).
The 2-D rater data is visualized using Matlab.

2.4.8 Building Top-Print

The Building Top-Print is a vector representation of the roof of the building. The roof of the building is represented as a polygon and the coordinates of the vertices are stored. This information can be used for modeling the buildings in an urban environment. The Building Top-Print information is obtained by manually editing the Flooded DEM using image-processing techniques. More details regarding building top- print information can be found in chapter 4.

2.4.9 Clutter Map

Yet another geographic data source that can be used for radio planning are clutter maps. The clutter map denotes the land activity or the density of the buildings at a particular area. The clutter map divides the area into different layers each with different building densities and land activities. Some propagation prediction tools use clutter data along with the terrain information to characterize the environment [15]. In some cases where the cost of high-resolution database is not justifiable, the clutter map can provide the sufficient information for propagation prediction [16].

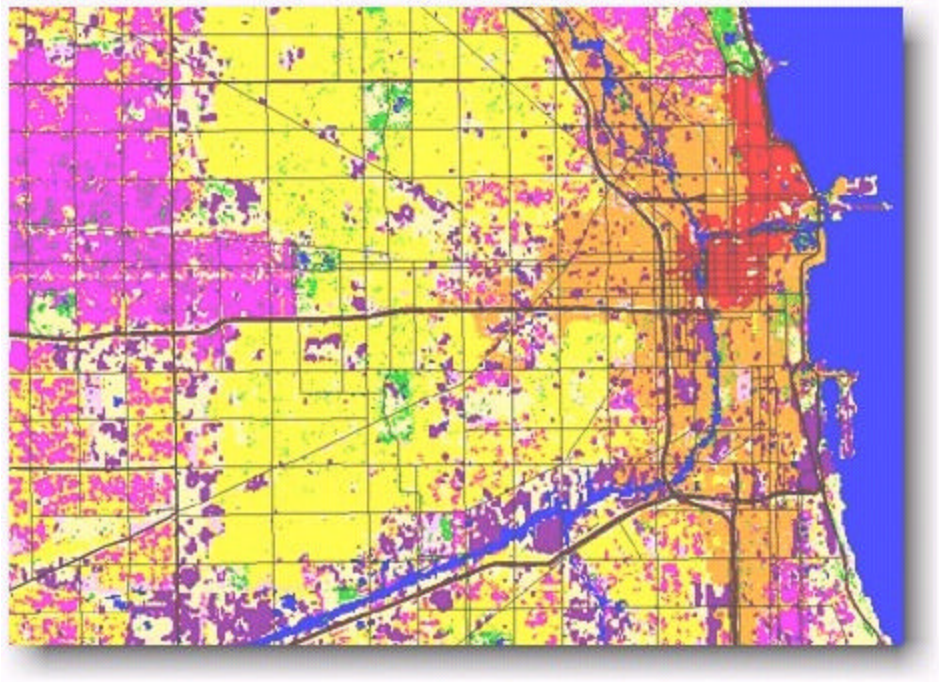

Figure 2.6: Clutter map of Chicago.
The regions in red,(darkest) show the highest building density and in yellow (lightest) shows lowest building density. (Source: I-cubed, Inc.).

2.5 Conclusion and Research Roadmap

The desirable characteristics of a database used to model the environment for a ray tracing based propagation prediction technique is presented in this chapter. The chapter also introduces the user to the various geographic data available in the market, which can be used to model the physical environment.

To model the environment for a propagation prediction tool, the buildings and the terrain have to be modeled from the geographic data available. Today's propagation prediction techniques use simple models to model the terrain and the buildings. This thesis proposes a method that can be used to model the terrain and the buildings, for a ray tracing based application, with the geographical information available today. Chapter 3 describes the different ways to model the terrain. It evaluates the different algorithms used to model the terrain and recommends a method best suited for propagation

prediction. Chapter 4 focuses on developing the methods that can be used to model the buildings and to combine the building information with the terrain information to obtain a comprehensive database of the environment.

Chapter 3

3 Terrain Modeling

This chapter discusses about the various issues pertaining to the modeling of the terrain for a site-specific propagation prediction algorithm. The different algorithms used to model the terrain are implemented and are evaluated thoroughly, keeping the ray tracing based application in mind.

3.1 Introduction

Most propagation prediction models assume a flat earth while predicting the performance of a wireless system. In contrast to this assumption, Vu-Dinh and Lampard [17] have proved that even moderate valleys and hills along streets would cause a considerable effect on the path loss. Over the years many researchers have proposed different strategies to account for the variability of the terrain. One of the earliest work in this area was done in Japan by Okumura, et. al. [18]. Okumura accounted for terrain variability by using a field strength correction factor. However, this technique is not site specific in nature since it does not allow for the evaluation of the signal for a specific location even if the terrain is known. W.C.Y. Lee introduced the concept of effective antenna heights to account for actual terrain variation [19]. There have also been studies to model the effect of shadowing of hills in the propagation characteristics of radio waves [20]. Bertoni and Piazza [21] have studied the effect of both buildings and the terrain on the signal and have come up with statistical models to estimate the signal strength. However, all the above mentioned research accounts for the terrain variability using statistical models.

Until recently almost all the ray optical methods modeled the terrain as a flat horizontal surface. However, recently, some of the ray optical models have started incorporating terrain in their propagation prediction technique [6]. The models, as described in [6] use the digital elevation data in the raster format, to represent the terrain and uses the elevation data directly for all the ray optical calculations. This raster data

generally occupies a larger storage area when compared to a vector database. Moreover, the raster data is not flexible enough to represent all the details of an object completely. For example, a raster data representation of the building cannot include the surfaces, which are inside the building and it is unable to model indoor-outdoor propagation using ray tracing techniques. Hence most ray tracing implementations prefer a vector database. Even though some reference have been made regarding the representation of the terrain in vector raytracing implementations such as [22], there have not been much study in the area of how to model the terrain for a ray tracing based application.

One of the earliest works to model the terrain for a ray optical based propagation prediction technique was done by Rajguru, et. al. in 1992 [23]. Rajguru uses a Triangular Irregular Representation (TIN) to model the terrain. The different algorithms to convert a Digital Elevation Model (DEM) to a TIN have been investigated. However, a thorough evaluation of the algorithms that can be used to model the terrain for a propagation prediction application is still missing. This chapter evaluates the different algorithms that can be used to model the terrain for a ray tracing application.

The first section of the chapter discusses the different ways of representing the terrain. One of the methods of representing the terrain is by using a DEM, which was introduced in the previous chapter. This chapter introduces a vector representation of the terrain called a Triangular Irregular Network (TIN). The chapter examines which representation is most suited for a ray tracing based application. The second section describes the different algorithms in the literature that can be used to convert the DEM to a TIN. These algorithms are implemented and the performance characteristics of the different algorithms are evaluated with the ray tracing application in mind.

3.2 Representing the Terrain

There are two fundamentally different ways to represent the terrain. The easiest and the most popular way to represent the terrain is as an array of elevations of a regularly spaced grid of points, popularly known as the DEM. Alternately, the terrain

can also be represented as a set of triangular planar surfaces, called a Triangulated Irregular Network or a TIN.

3.2.1 Digital Elevation Model

Digital Elevation Models represent the terrain as a 2-D grid of elevations of regularly spaced points of an area. The elevations of the same latitude are arranged row wise and the elevations of the same longitude is arranged column wise. As mentioned in Chapter 2, Digital Elevation Models (DEMs) of most of the urban and sub-urban regions of the US of A, are readily available from various private and public sources. The DEM data format is simple and easy to manipulate. However, DEMs suffer from data redundancy while representing uniform terrain. Moreover, the DEM is in a raster format. Most of the propagation prediction tools requires a vector format for representing the terrain.

3.2.2 Triangulated Irregular Network (TIN)

The TIN model was developed in the early 1970's as a simple way to build a surface from a set of irregularly spaced points. The Triangulated Irregular Network (TIN) model of the terrain consists of a non-overlapping network of planar triangular polygons based on irregularly spaced nodes [10]. The irregularly spaced node refers to the fact that no three nodes in the TIN model are collinear.

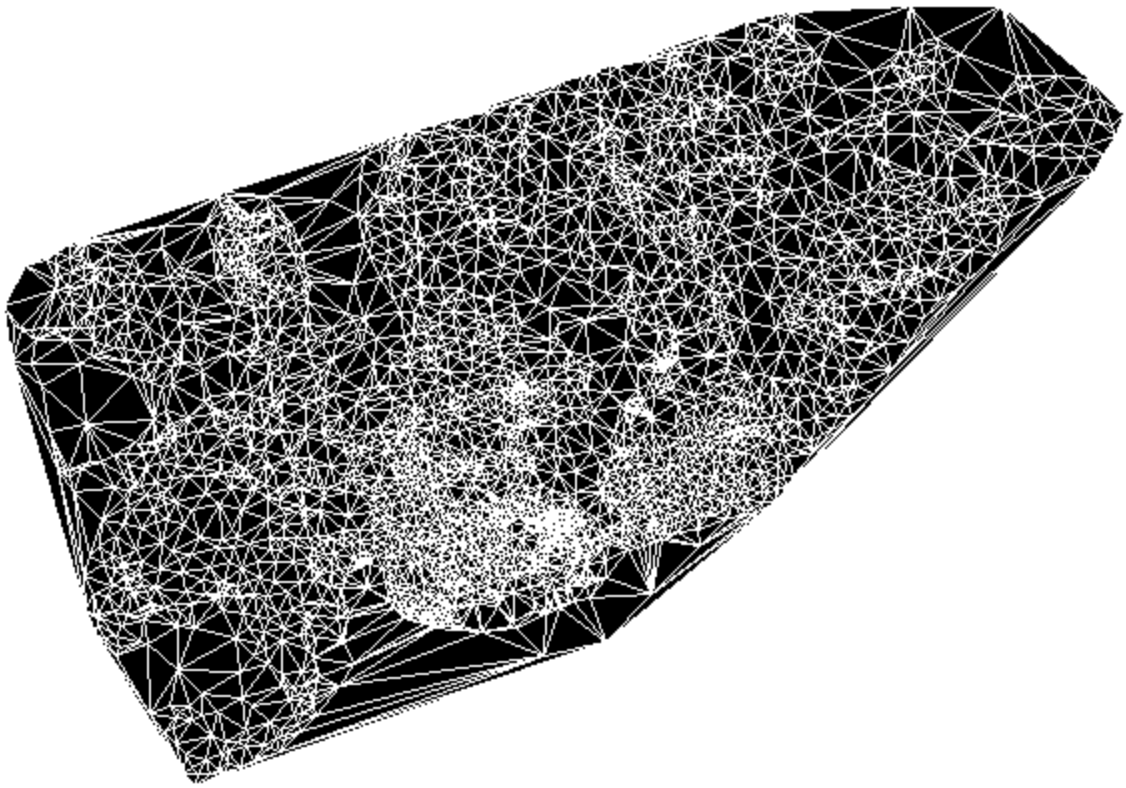

Figure 3.1: A Triangular Irregular Network of Toronto. (Source:http://www.eng.upm.edu.my/~rodzi/notesonline/kaw3502/4.3D_Visualisation/tin.html)

The TIN is a vector topological structure since only the set of nodes and the set of straight lines interconnecting the nodes need be stored. The TIN implementation can be made efficient by placing a larger number of nodes in the areas of rough terrain and fewer nodes in smooth terrain. The areas with relatively flat terrain can be modeled by using large triangles and with rough terrain can be modeled using smaller triangles. This makes the TIN model very efficient in terms of the size of the database. As the number of surfaces must be modeled to represent the terrain decreases, the computational complexity of the ray tracer also decreases drastically. Therefore, the TIN model is a very good candidate for modeling the terrain for the site-specific propagation prediction software [23].

3.2.3 Conversion of DEM into TIN

Unlike the DEM files, which are readily available from different vendors, the terrain data is not readily available in the form of a TIN. The DEM has to be converted into the TIN format. The rest of this chapter concentrates on evaluating the different techniques that can be used to convert a DEM into a TIN format, keeping a ray tracing application in mind.

A straightforward method to convert the DEM into a TIN would be to use all the points in the DEM as nodes of a TIN and connect the all the nodes with its two neighbors to from a network of triangles. However, such an implementation would result in a large number of triangular surfaces in the TIN. Consider for example, a DEM, with a 1m x 1m resolution for an area of 1sq km. Such a DEM would consist of 1000 x 1000 points. A TIN model with all points of the DEM as nodes of a TIN would require approximately 0.5×10^6 surfaces to model the terrain. The complexity of the ray tracer increases exponentially with the number of surfaces to be considered. A TIN representation with 0.5×10^6 surfaces would increase the computation time many fold.

For efficient performance of ray tracing based propagation prediction software, the number of surfaces used to model the environment should be minimized. To decrease the number of surfaces used to model the terrain, the uninteresting points of the DEM need to be filtered out and only the interesting points should be used to develop the TIN. However, the elimination of the points from the DEM while representing the terrain in TIN format would cause errors in the TIN model.

There are several metrics used to compare the numerical accuracy of the TIN model with the DEM used to create it. Accuracy is usually measured by comparing the elevation of a point in the DEM with the elevation of the point as represented by the TIN. The difference in the elevations is called the error of the point. The metrics that have been used in the past include the total error, the maximum error and the mean and the standard deviation of the error [24]. For our purpose we choose the maximum error as the

metric while comparing the different algorithms used to convert a DEM to the TIN. A TIN with a maximum error less than a particular value would ensure that all the points in the DEM has an error less than that value. Note that all the DEMs would have a minimum resolution while representing the elevation for the sample points. Therefore, a TIN representation of a DEM with a maximum error less than the minimum resolution of the DEM can be considered as practically 'error free'.

3.3 Techniques for Converting DEMs to TINs

Over the years researchers have simulated the different ways of converting a DEM into a TIN [25][26]. Most of the algorithms use a common approach while developing the TIN model from the DEMs. First a few 'significant' points of the DEM are identified. Here, 'significant' point refers to those points that are most useful in describing the surface and bringing out its salient topological features such as sharp variations. These points are then triangulated using triangulation algorithms to make the TIN model of the terrain. But recently, a different approach, which integrates the point selection and the triangulation algorithm, has been reported [27].

3.3.1 Selecting the Points

Several algorithms have been proposed to select the 'significant' points from the DEM with minimal loss of information about the terrain [25], [26]. These methods differ in the criteria used to select the points in the DEM. Some of these methods are used in popular terrain mapping software like ARC/INFO [28].

3.3.2 Fowler and Little algorithm

According to the Fowler and Little algorithm [25], only the points that represent significant characteristics of the terrain such as peaks, pits, ridge lines and channel lines are chosen from the DEM. The TIN is created by connecting these sets of points using triangulation algorithms. The Fowler and Little's algorithm is described in detail below.

The Fowler and Little's algorithm compares each point in the DEM with its eight immediate neighbors to decide whether to ignore the point or select the point for triangulation. The eight immediate neighbors of a point in the DEM, with x coordinate i, and y coordinate j, are (i ,j-1), (i-1, j-1), (i+1,j-1) , (i-1,j), (i+1,j), (i-1,j-1), (i+1,j) and (i+1,j+1) (Fig. 3.2).

i+1,j-1	i+1,j	i+1,j+1
i,j-1	i,j (central point)	i,j+1
i-1,j-1	i-1,j	i-1,j+1

Figure 3.2: The central point with its eight neighbors

The eight neighbors of each point are labeled '+' if the elevation of the point is greater than that of the central point and '–' if the elevation is less than that of the central point. A point is considered as a 'peak' if all the neighbors have a lower elevation when compared to the central point, i.e. if all the neighbors are '-' s. The point is considered a 'pit' if all the neighboring points have a higher elevation when compared to the central point, i.e. if all the neighbors are '+' s. If a path can be traveled around the central point to all its contiguous neighbors in a clockwise or anti clockwise direction such that the +'s and the –'s oscillate between each other at least twice, then the point is ignored from the DEM (Fig. 3.3). The rest of the points are retained and used for triangulation.

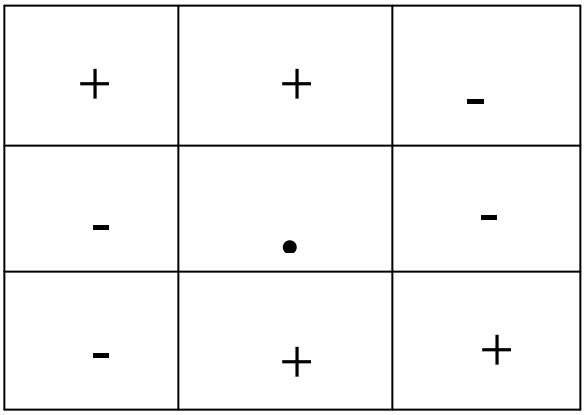

Figure 3.3: Two complete cycles for Fowler's Algorithm
Note that by travelling in a path around the eight surrounding points, around the central point, the +' s and the –'s oscillate over two complete cycles.

The Fowler and Little's algorithm is found to suit only certain types of landscape [29]. It works well for landscapes with many sharp breaks of slopes, ridges and sharp channels. The algorithm may not work well for an urban scenario, where there are not many peaks and pits or ridges. The DEM can only be roughly approximated using Fowler and Little's algorithm. Moreover, the error in approximating the DEM into a TIN would be different for different kind of landscapes. In other words, the Fowler and Little's algorithm cannot be used for TIN modeling, where a maximum error has to be maintained. So this approach is not suitable for propagation prediction, especially for urban and semi urban areas since it can cause significant errors while doing propagation prediction for certain types of landscapes.

3.3.3 Very Important Points (VIP) Algorithm

The VIP algorithm uses a different criterion to determine whether the point has to be ignored or whether it has to be retained from the DEM while constructing a TIN [26]. The VIP algorithm assigns a certain 'measure of significance' for all the points in the DEM, based on the difference in elevation of the pixels with its neighbors. All the points with a 'measure of significance' below a certain threshold are ignored while triangulating

the DEM. This is a simplification technique used in a popular terrain mapping software called ARC/INFO [28]. The VIP algorithm is explained in detail in the next paragraph.

According to this approach, each elevation point is considered with its eight neighbors, which forms four diametrically opposite pairs, i.e. up and down, right and left, upper left and lower right, and upper right and lower left. For each point, each of these pairs of neighbors is examined in turn. The diametrically opposite neighbors are then connected by a straight line, and the perpendicular distance from the central point to this line is computed. Fig. 3.4a shows the elevation of a central point and it's eight neighbors. Fig. 3.4b shows how the perpendicular distance from the central point is computed between the upper left and lower right points. The average of the four perpendicular distances is computed and it is called the 'measure of significance' of the point. The 'measure of significance' for all the points in the DEM set is computed. The points are deleted from the DEM in the order of increasing significance, deleting the least significant first. This is continued until the number of points reaches a pre-determined limit or the 'measure of significance' is above a certain threshold. The undeleted points are then used for triangulation to get the TIN representation of the terrain.

10	9	8
6	6	8
7	5	8

Figure 3.4a: The central point and neighbors with the elevations

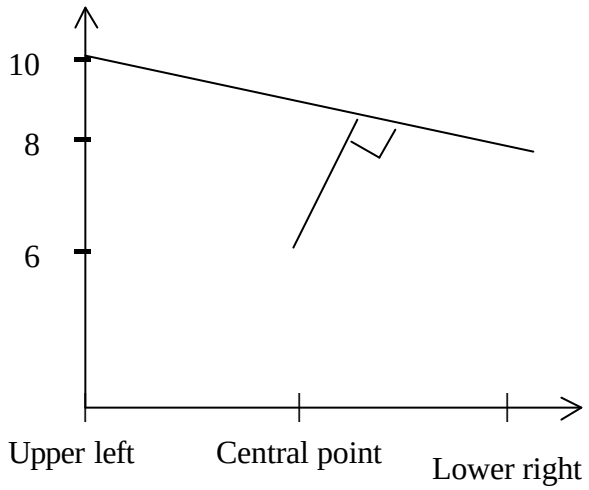

Figure 3.4b: Finding the perpendicular distance from the central point to the line connecting diagonally opposite neighbors

This process gives a more accurate representation of the terrain when compared to the Fowler and Little's algorithm [25]. However, even this algorithm would not ensure that the maximum error of a DEM dataset, when represented using a TIN model is below a certain value. Therefore, even though this method may give a more accurate representation of the terrain in most places, it may cause significant errors in some other regions.

The VIP and the Fowler and Little's algorithm filters out the points that represent the significant features of the terrain. These points should then be connected together to form a set of solid planar triangles that represent the terrain.

3.4 Triangulation Algorithms

Triangulation is a process of interconnecting a set of points to form non-overlapping triangles. There have been several different triangulation algorithms that have been reported. [30], [31]. Delaunay Triangulation algorithm and the Radial Sweep Algorithm (RSA) are the two most widely used triangulation algorithms. Different triangulation algorithms differ from each other in the number of triangles created for a

given set of points, the quality of the triangles (whether they are short and fat or long slivery) and the computational complexity of the algorithm. The quality of the triangles produced is generally measured by the maximum distance of any point inside a triangle from a vertex [32]. The resultant triangular network should ideally contain short, fat triangles that are as close to equilateral as possible, as opposed to long slivery triangles. This ensures that the interpolations done on these triangles are valid and are dependent on closer points than far out points. The triangulation algorithm should be computationally inexpensive and should not contain any redundant information.

The Delaunay triangulation algorithm has several desirable characteristics. The Delaunay Triangulation algorithm creates fat, short triangles and the triangulation algorithm is incremental in nature [31].

3.4.1 Delaunay Triangulation Algorithm

The Delaunay triangulation algorithm [31] is named after a Russian mathematician B. Delaunay, who developed it at the turn of the twentieth century. The Delaunay triangulation algorithm converts a given set of points into a network of non-overlapping triangles such that no point in the network is enclosed by the circumcircle of any triangle. A circumcircle of a triangle is defined as a circle that passes through all the three vertices of the triangle. The 2-D Delaunay triangulation algorithm is explained in detail below.

Consider a set of points (a dataset) that has to be represented as a network of triangles. First, three imaginary points, which correspond to the vertices of an imaginary triangle, which enclose the whole dataset, are computed. Each point of the data set is then added to the imaginary triangle incrementally and a new set of triangles are computed. The incremental algorithm for adding a new point to the Delaunay triangulation network is explained below.

Consider eight points as shown in Fig. 3.5, which are already connected using a triangular network with seven triangles. Figure 4.5 also shows the circumcircles of the seven triangles in the triangular network. Assume that in the next iteration a point P9 has

to be added. Then the Delaunay algorithm operates according to the following procedures.

1) Determine the circumcircles that contain the new point. In this example, they correspond to three triangles, P1P2P5, P1P5P6 and P1P6P3.
2) Make a list of all edges of those triangles: P1P2, P1P5, P2P5, P1P5, P1P6, P5P6, P1P6, P1P3 and P6P3.
3) Delete any edges that appear more than once. Edges P1P5 and P1P6 are deleted in our example. Create a 5-sided polygon as in Fig. 3.6.
4) Connect the new point P9 to the vertices of the new polygon. The five edges P9P1, P9P2, P9P3, P9P5 and P9P6 are constructed, which creates five new triangles in Fig. 3.7.

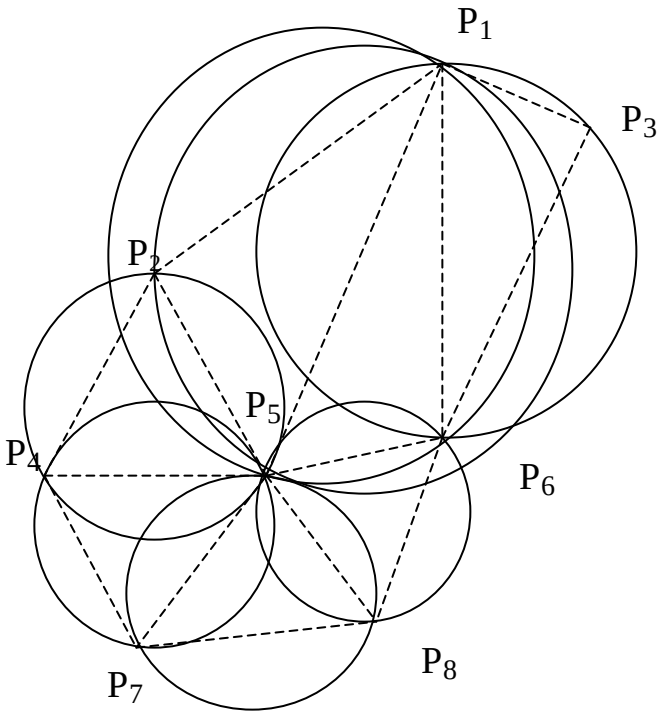

Figure 3.5:The eight points which make seven triangles and their circumcircles of the triangles

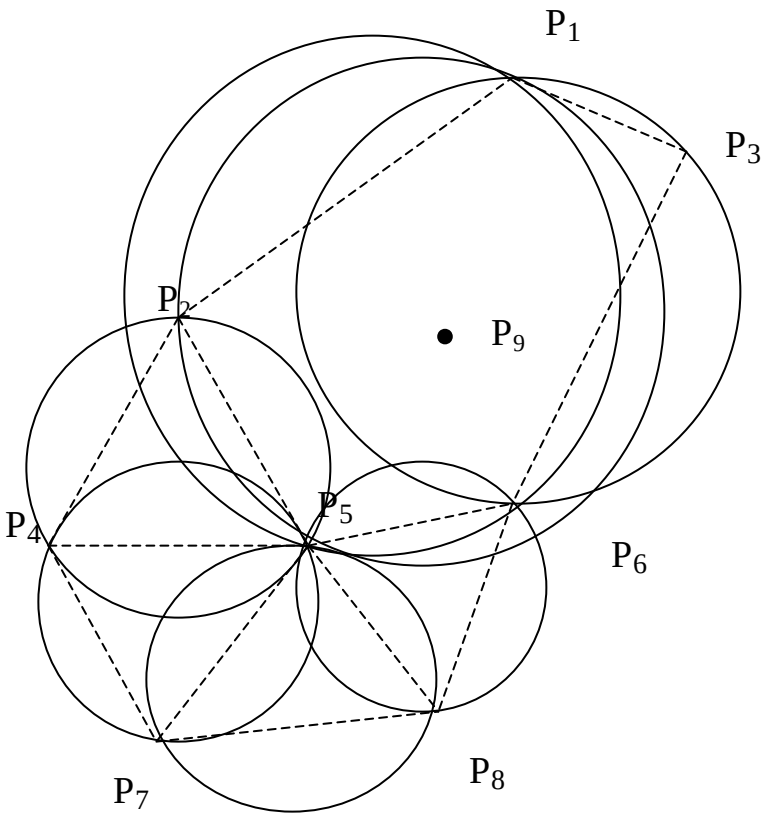

Figure 3.6: Addition of a new point in triangular network.

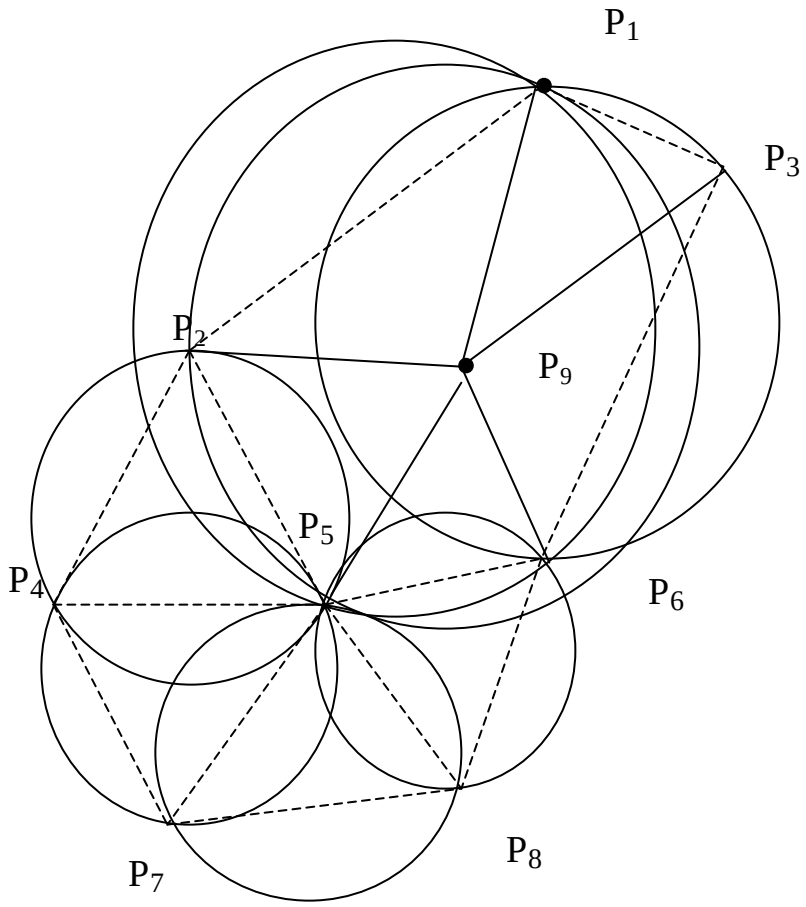

Figure 3.7: Addition of a new point in triangular network

5) This is carried out until all the points in the data set are added to the triangulation algorithm.

The Delaunay triangulation method has several desirable properties:

1) If the algorithm joins three points in a triangle, no other point will be located inside the circumcircle of the triangle.
2) Given four neighboring points that define a quadrilateral, this quadrilateral is split, in one of the loop iterations, in a way that maximizes the smaller of the internal angles. The algorithm does not create thin wedge like triangles if at all possible.

3) The triangulation is unique.
4) In cases where there are regions of points with high density and a region of points in low density, this triangulation method produces more number of triangles in the former case and lesser number of triangles in the latter.

But the Delaunay triangulation algorithm may fail in certain degenerate cases:

1) Any two points are identical
2) Any three points in the data set are collinear.
3) Any four points in the data set lie on a circle.

Delaunay triangulation as explained above deals with points in a two dimensional plane.

This technique can be extrapolated to the three dimensional DEM of a particular region. The Delaunay triangulation algorithm operates on the selected points in the DEM after filtering the points using the Fowlers and Little's algorithm or the VIP algorithm.

A different approach used for the extraction of TIN from a raster database is obtained by integrating the point selection and the triangulation method. DeFloariani, et. al. have proposed a hierarchical algorithm, which integrates the point selection algorithm with triangulation [27]. Another method, mentioned in [33], integrates the point selection algorithm with the Delaunay triangulation algorithm form a TIN.

3.5 Hierarchical Triangulation Algorithm

The Hierarchical Triangulation method was proposed by Floriani, et. al, as a generic method to model 3-D surfaces from a 3-D raster database. This method can be easily adapted to model the terrain. The hierarchical triangulation method uses a hierarchical structure based on nested triangles for triangulation [27]. The triangles are hierarchically subdivided into nested triangles in such a way that the maximum error of the DEM is minimized at each stage. This algorithm allows the user to model a surface for any desired maximum error. The algorithm is described below.

Initially the whole DEM data set is enclosed in an imaginary triangle as shown in Figure 3.8. The initial triangle is considered to be the root of a tree. Note that the initial triangle is a three-dimensional triangle with X, Y and Z coordinates. If the X-Y projection of the points is enclosed by the X-Y projection of the triangle, these points are said to be 'enclosed' by the triangle. The difference in elevation of each data point in the DEM to that of the triangular surface that approximates it is called the 'deviation' of the point (Fig. 3.9). The deviation of the point is a measure of the error in representing of a point in a TIN when compared to the original representation in a DEM. The maximum of the deviation is nothing but the maximum error of the TIN model.

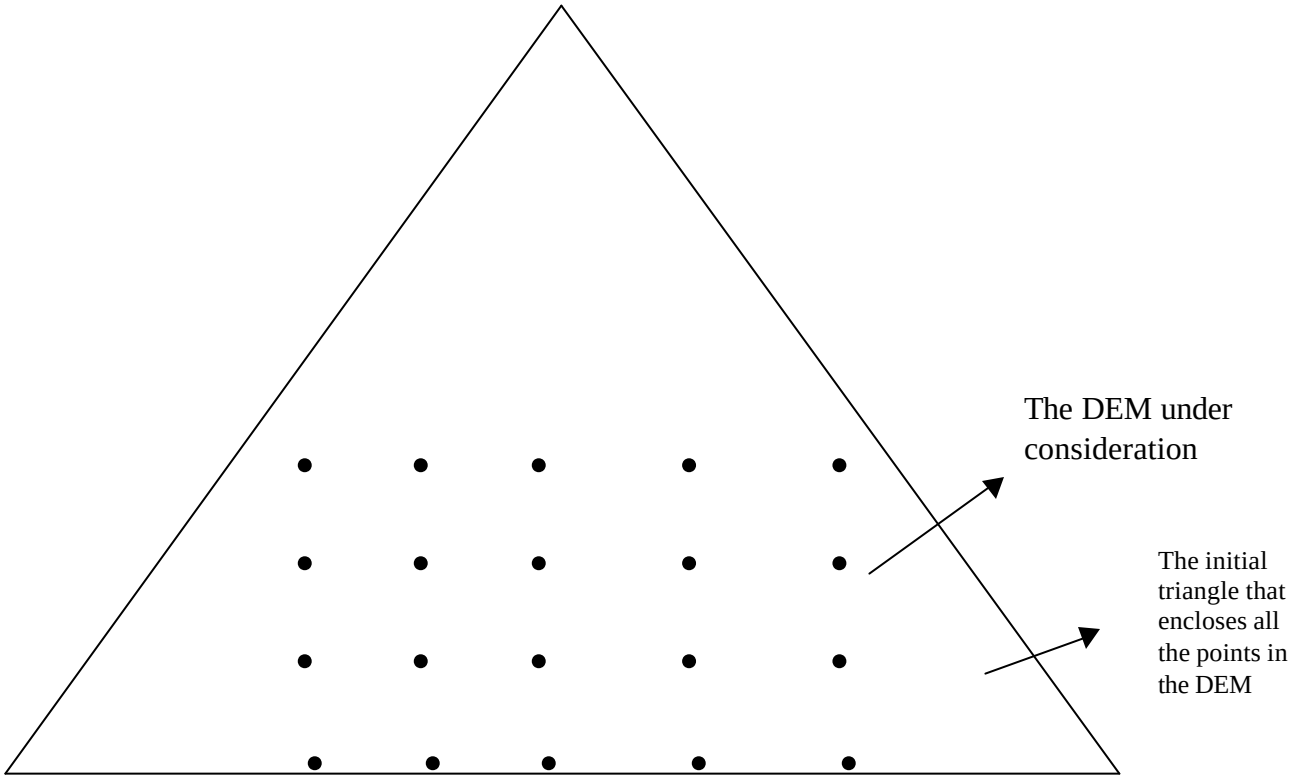

Figure 3.8: The initial triangle that encloses all the points in the DEM

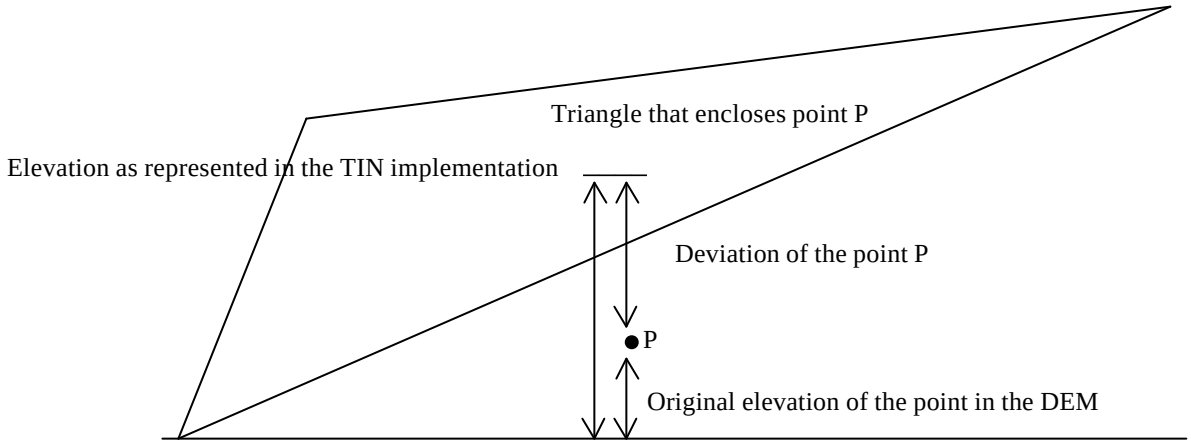

Figure 3.9: The deviation of the points when the TIN is compared to the DEM.

As a first step, the initial triangle is considered and the procedure operates on this triangle as follows.

1) The deviations of all the points enclosed by the triangle under consideration are computed. The one with the maximum deviation is added to the set of points to be triangulated. For example let P4 is the maximum deviation point which is enclosed in the triangle P1P2P3 (Fig. 3.10).
2) The triangle is then subdivided into three nested triangles with the maximal deviation point (P4) as one of the vertices of all the three triangles (Fig. 3.11). The three resulting triangles are then considered as the children of the parent triangle.
3) One of the new triangles created is then considered. Steps 1 and 2 are carried on until all the points of the triangle have a deviation less than some specified value. This value would be equal to the maximum error of the dataset.
4) This is carried out until all the triangles in the ‘leaf’ nodes of the tree structure have a maximum error less than the desired value. The node with no children is called the ‘leaf node’.

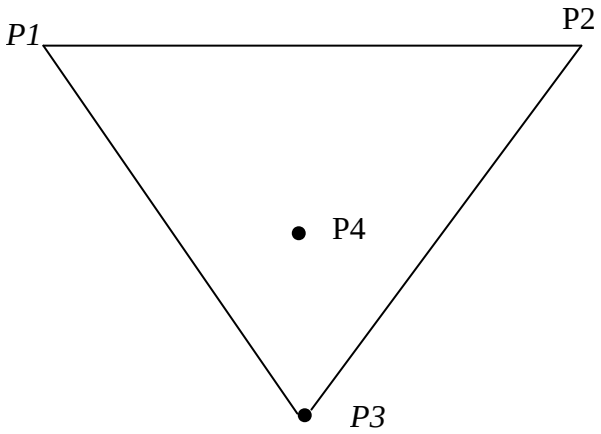

Figure 3.10: Addition of the point P4, into the triangle P1P2P3

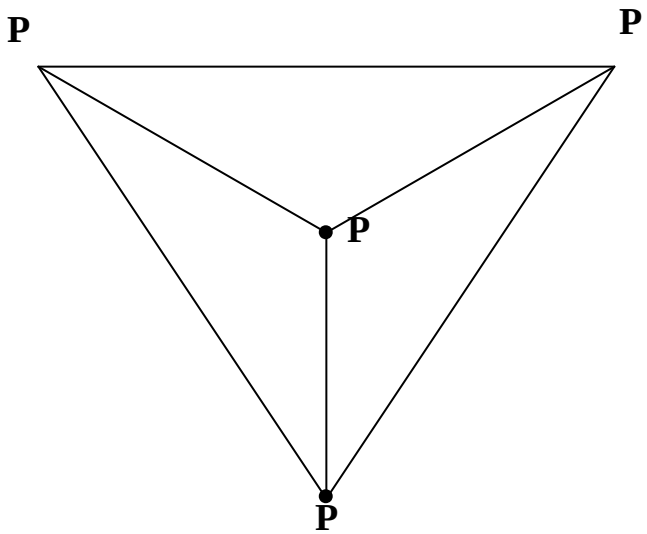

Figure 3.11: Addition of the point P4 by splitting the triangle P1P2P3.

By using the hierarchical triangulation algorithm, each triangle is split locally into three triangles, each time a new point with a deviation greater than the required

maximum error is encountered. To improve the efficiency of the hierarchical algorithm, all the points in the DEM, which are enclosed in the triangle can be stored along with the data structure that represents the triangle. As the triangle is divided into smaller triangles, only the points that are enclosed by the parent triangle need to be checked for 'enclosure' with the resulting three smaller triangles. This is found to improve the computational speed by a significant factor. The Hierarchical triangulation algorithm allows the user to specify a certain maximum error for the data set. This allows the user to model the TIN of the terrain with any arbitrary resolution.

3.6 Iterative Delaunay Triangulation Algorithm

Yet another method to convert a DEM into a TIN is by iteratively using the Delaunay Triangulation algorithm along with the picking of the points from the DEM [33]. This method has the advantages of the Delaunay triangulation algorithm which results in short fat triangles and the integrated point picking method, which allows the user to develop a TIN representation with a given maximum error. A user, who needs only a rough approximation of the terrain, can choose a large value as the 'maximum error'. This would make the number of surfaces used to represent the terrain a minimum. To get a more accurate representation of the triangle, the user can choose a very low value as the 'maximum error' and model the terrain accordingly. The algorithm is described in detail below.

As in the hierarchical algorithm, three imaginary points are computed so that all the data points in the DEM are included in an imaginary triangle defined by these three points as vertices (Fig. 3.8). The method proceeds as follows;

1) The deviation for all the points in the DEM data set is computed.
2) The point with the maximum deviation is then added to the set of points to be triangulated.
3) The standard 2-D Delunay triangulation algorithm is carried out with the X-Y projections of all the points now included in the triangulation algorithm. After the

2-D triangulation is carried out, the Z coordinates of the vertices of the triangles are added. This makes the triangles three-dimensional.

4) The steps 1 through 3 are carried out until the deviations of all the points in the data set of the DEM are below a certain threshold. Note that this threshold would be the required maximum error of the DEM. So using this method, the maximum error of the TIN representation can be controlled directly. Note that all the DEMs would have a particular resolution in elevation associated with them. The maximum error is generally taken as a number greater than the resolution of the DEM.

Note that the DEM consists of a grid of points, which are collinear to each other. The Delaunay algorithm fails if any three points are collinear to each other. The X and the Y coordinates of each of the points are added by a very small random number to make the points non-collinear. The error introduced due to this is assumed to be minimal provided that the maximum random number that is being added is much less than the minimum horizontal or vertical resolution of the DEM. In the current implementation, the random number is generated using a uniform random number generator, which has a maximum value equal to 0.1.

Like the Hierarchical triangulation algorithm, the Delaunay based algorithm also allows the user to model the terrain with any arbitrary resolution. The Delaunay triangulation algorithms produce short and fat triangles and also produce a lesser number of triangles when compared to the hierarchical algorithm. However, while using the Delaunay triangulation algorithm, the point that has to be incrementally added to the TIN, has to be compared with the circumcircles of all the triangles in the TIN network. This makes the Delaunay based triangulation method computationally expensive when compared to the hierarchical model, especially when there are a large number of triangles in the TIN.

3.7 Parallel Implementations of the Algorithms

The hierarchical algorithm can be easily implemented in a parallel fashion. Each of the triangles can be checked for the maximum deviation point in a parallel fashion. Every time, a triangle is split into three different triangles, three new processes can be forked. Each of the processes can deal with the three different triangles that have been produced. This is not possible using the Delaunay triangulation method because the splitting of the triangle is not local. Every time a new point is added to the TIN, the whole of the TIN network is changed.

3.8 Comparison of the Algorithms

The Very Important Points algorithm, Delaunay based Triangulation algorithm and hierarchical triangulation algorithm is executed for a Bald Earth DEM for the city of Denver. The horizontal resolution of the DEM is 5m x 5m. The vertical resolution is 1m. Therefore, a TIN implementation with a maximum error of 1 meter can be considered as practically 'error free'. A grid of 200 x 200 points is considered. For the Very Important Points algorithm, the 'threshold of significance' is taken as 1 meter. Both the Hierarchical triangulation algorithm and the Delaunay based algorithm has a threshold of 1 meter. The computation time is also measured for each algorithm.

Algorithm	Computation Time in sec	Number of Triangles	Number of points with error greater than 1 meter	Maximum error
VIP points (threshold = 1m)	1 sec	8	14457	2.2308
VIP points (threshold=0.5m)	1 sec	30	7442	2.77326
VIP points (threshold =0.25m)	78	601 0	77	1.7179
Delaunay based Algorithm	69	146	0	< 1 (error free)
Hierarchical	21	240	0	< 1 (error

algorithm				free)

Table 3.1: Comparison of the different DEM to TIN algorithms with the Denver database

When the Very Important Points algorithm with a 'threshold of significance' of 1 m is used, the number of triangles in the TIN are very less (8). But there are significantly large number of points which have point error greater than 1. So the 'threshold of significance' is lowered to 0.5 and then to 0.25 to decrease the number of points that has an error greater than 1. When the threshold of significance is made 0.25 meters, a fairly large number of triangles (6010), are required to represent the DEM. Using Delaunay based triangulation algorithm, the number of triangles in the TIN representation is very less (146) when compared to VIP points algorithm with threshold = 0.25. There are no points above error = 1. The Hierarchical triangulation algorithm takes significantly lesser time when compared to Delaunay triangulation algorithm. But the number of triangles nearly doubles.

A similar experiment is conducted with the Bald Earth DEM of the city of Chicago. The results are presented below.

Algorithm	Computation Time in sec	Number of Triangles	Number of points with error greater than 1 meter	Maximum error
VIP points (threshold = 1m)	1 sec	24	14457	3.98109
VIP points (threshold =0.5m)	5 sec	146 8	3224	3
VIP points (threshold = 0.25 meters)	81	606 0	344	1.5807
Delaunay based Algorithm	262	348	0	< 1 (error free)

Hierarchical algorithm	129	103 6	0	< 1 (error free)

Table 3.2: The comparison of various DEM to TIN algorithms with Chicago database

Even though, the number of triangles for the Chicago database was found to be higher than the Denver database, the relative performance between the algorithms remains more or less the same.

From the above experiments it is clear that either the Delaunay based triangulation algorithm or the hierarchical triangulation algorithm are most suited for TIN development. The Delaunay triangulation algorithm can be used for smaller databases, since it produces lesser number of surfaces and is executed in a reasonable amount of time. The Hierarchical triangulation algorithm can come in handy for large databases and where parallel processing can be employed.

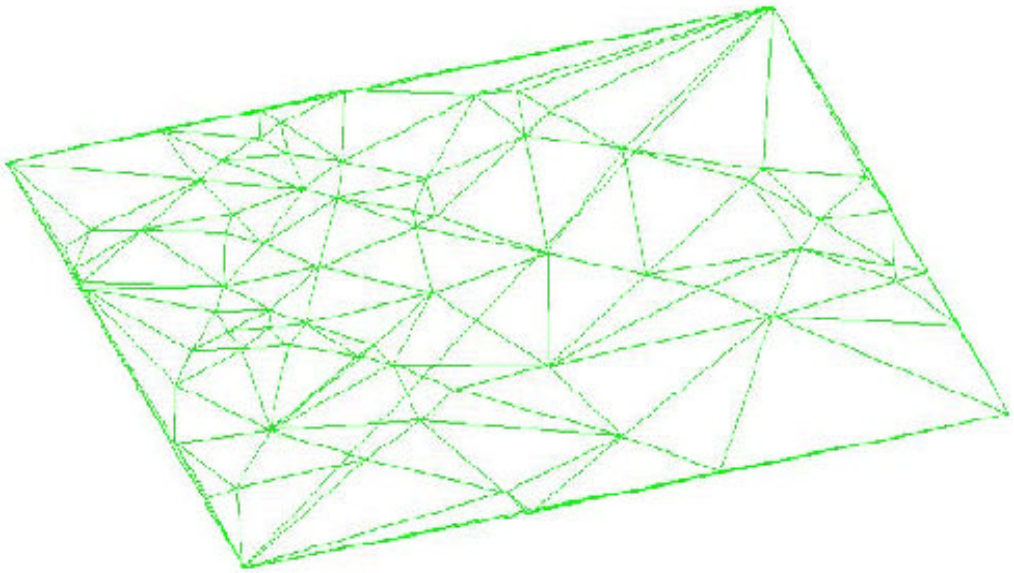

Figure 3.12: The TIN representation of a real terrain using Delaunay based triangulation algorithm (Denver, CO)

3.9 Accelerating the Iterative Delaunay Triangulation Algorithm

The Delaunay based triangulation algorithm has a complexity equal to O (n^2) [31]. This means that as the number of points in the DEM data set doubles, the computational complexity increases four times and so on. Therefore, the Delaunay-based algorithm would not be practical as the number of points in the DEM increases. So to improve the computational speed of the algorithms, the entire DEM grid can be divided into different areas with lesser number of points. The triangulation algorithm can be carried out in those areas separately. Even though this would make the algorithm sub-optimal, it would decrease the computation considerably. For example, a DEM with 1000 x 1000 points can be split into 25 sub areas with 200 x 200 points each and the triangulation algorithm can be carried on with it. The total computation time with 25 (200 x 200) points was found to be 20 minutes and the total number of triangles in the TIN equal to 2513 triangles.

3.10 Chapter Summary

This chapter discusses about the different ways of representing the terrain for propagation prediction. A Triangulated Irregular Network (TIN) model is found most suitable for the Site specific propagation prediction software. This chapter discusses about two different approaches that have been used for extracting the TIN from a DEM. One class of algorithms, filter the data available and picks only the significant points from the DEM. Triangulation algorithms are then used to develop the TIN with these points. Yet another class of algorithms integrates the picking of the points with the triangulation algorithms. The second approach is more suitable for a ray tracing based software since this approach allows the user to model the TIN with a certain Maximum error. Two algorithms, which use this approach, are presented. One based on Delaunay triangulation method and another one based on hierarchical structures. The above mentioned algorithms are executed on a DEM and the statistics of the results are

presented. It has been found that the Delaunay-based Triangulation algorithm models the TIN with the least number of triangles. A method to improve the computational complexity of the Delaunay based algorithm is also presented.

Chapter 4
4 Modeling the Building Database

This chapter concentrates on the aspects related to the modeling of the building database and combining the building information with the terrain information.

4.1 Introduction

A deterministic propagation prediction technique based on ray tracing requires a full 3-D vector database of the buildings in the environment for an accurate prediction of the propagation characteristics. However, many practical rays tracing implementations still use 2-D building layout [34], [35] while modeling the buildings. Some implementations assume that all the buildings are of the same height [36]. These assumptions would restrict the use of ray tracing based prediction models to certain types of applications. For example, a prediction technique based on 2-D ray tracing can only be used if the base station height is lesser than the heights of the buildings surrounding it [5]. For a ray-tracing based prediction model to be versatile in its application and accurate in prediction, a 3-D vector model of the building database is essential.

Unlike the 2-D building layouts that can be directly obtained from city maps, the 3-D vector database of the buildings are not readily available. Some of the earlier works by Schaubach, et. al. [37] and Landstorfer, et.al. [36] introduces some aspects of designing a full 3-D building database. Schaubach mentions that buildings can be modeled, as convex polygons comprised on individual planar panels. Landstorfer assumes that all the buildings have a constant height and have flat rooftops. Until recently, the non-availability of high-resolution geographic data was the main stumbling block in modeling a building database. However, today with the availability of the new geographic products such as building top-prints and building foot-prints, accurate modeling of a 3-D building database for an urban or a sub urban environment can be achieved. The buildings and the terrain information, typically obtained from disparate sources, need to be integrated together in a format that the propagation prediction

software can use for analysis. This chapter focuses on the different aspects of modeling the building database from currently available geographic products and the integration of the building data with the terrain information.

The first part of the chapter discusses the geographic products currently available that can be used to model the buildings. The next section presents an algorithm that can be used to convert the available data format into a full-scale 3-D vector database of the buildings. The latter part describes the method used to integrate the building data with the terrain information.

4.2 Building Top-Print

Most site-specific propagation prediction tools require a vector input for the building database. One of the data that can be used while modeling the buildings is called a building top-print. Top-prints of buildings are vector files that represent the rooftops of the buildings and can be purchased from private vendors such as I-Cubed Inc. The different buildings in the building top-prints are indexed using a unique building number. Each building rooftop has its own a unique rooftop index number associated with it. Information regarding the mapping of the rooftop index numbers to the building index numbers is stored in a separate file. The building rooftops are modeled as horizontal polygons with the X and Y coordinates stored in an anti-clockwise direction. The elevation of each of the roof top polygons as measured from the sea level is stored along with each ceiling information. The rooftop polygons can have any number of sides according to the shape of the building being modeled. For example, consider a cubic building with four vertical walls and a horizontal roof associated with it (Fig. 4.1).

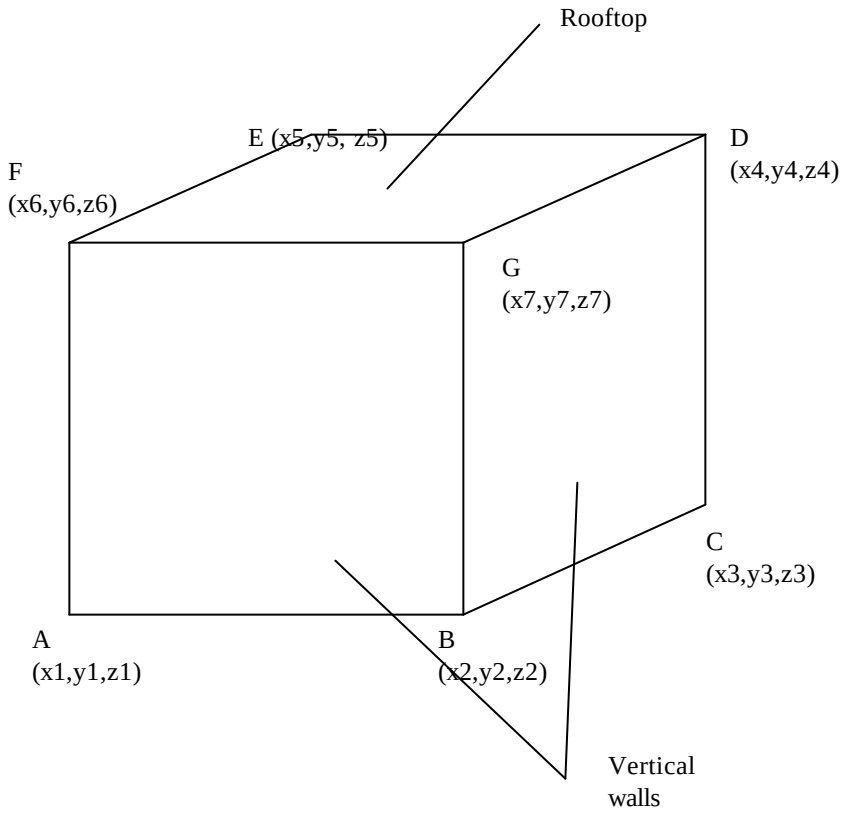

Figure 4.1: A rooftop polygon of a simple cube shaped building

For a building similar to Figure 4.1, the top-print of the building would have the X and Y coordinates of the roof polygon GDEF and the elevation of the rooftop polygon above sea level is stored along with the rooftop information. Note that the building top-print information does not include any information regarding the vertical walls of the buildings and this has to be modeled separately.

For a building with a sloped roof, the building is approximated as having a number of horizontal roofs which has different elevations which range from the minimum elevation of the sloping roof to the maximum elevation (Fig. 4.2). The top-print of the building is approximated as a series of concentrated horizontal rooftop polygons with different elevations associated with it.

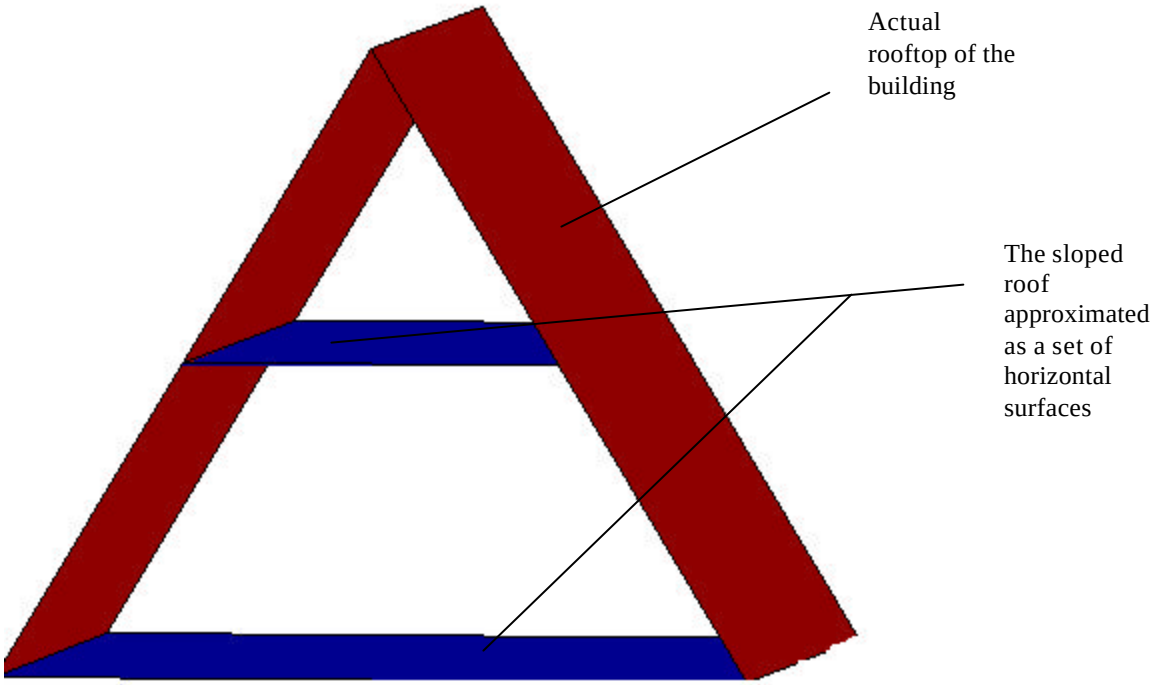

Figure 4.2: A sloped roof building and its rooftop polygons

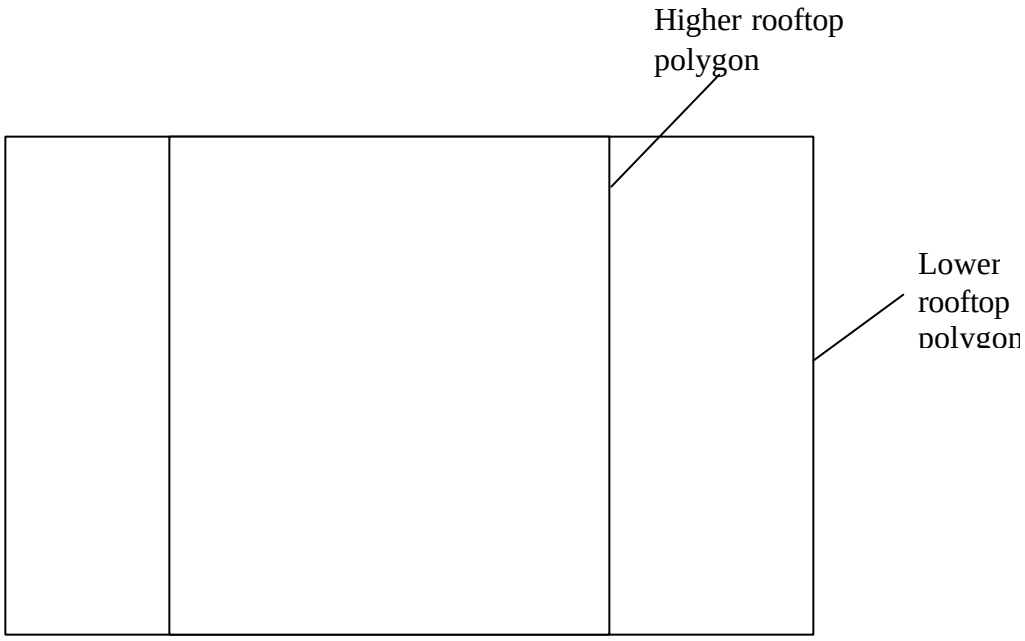

Figure 4.3: the building top-print of the building shown in Figure 4.2.

(as seen from a top view)

In the case where the building has different elevations associated with it (like the Empire State Building), the top-print model of the model consists of three concentric rooftop polygons each with different elevations associated with it. Consider a building, which has three elevations h1, h2 and h3 as shown in Figure 4.4. The top-print information would consist of three polygons and the elevations h1, h2 and h3 associated with each of these polygons.

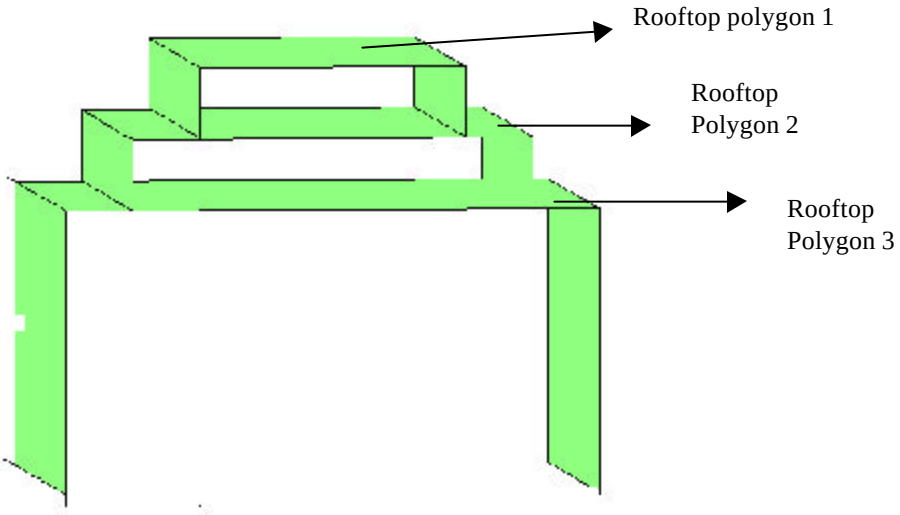

Figure 4.4: The rooftop polygon of a building with three heights.

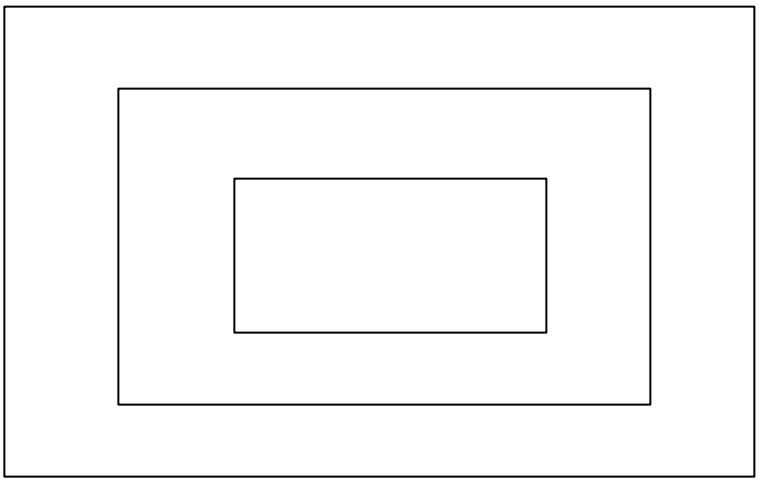

Figure 4.5: The top-print information of the building as shown in Figure 4.4 (as seen from a top-view)

4.3 Modeling the Buildings

The building top-print information and the building foot-print information are used to model the buildings. The building foot-print models the foot-prints of the exterior walls of the buildings and also provides the elevation of the base of the building. The buildings are modeled as a set of horizontal and vertical flat polygonal surfaces.

The top-print information of the building represents the building rooftop as a single or concentric horizontal polygonal surface with arbitrary number of sides as determined by the shape of the building. The rooftop is modeled as a horizontal polygonal surface with the X, Y and Z values of the vertices as obtained from the building top-print information. The vertical walls of the buildings are modeled as rectangular vertical polygonal surfaces. A rectangular vertical polygon is created for each edge of the rooftop polygon. A vertical rectangular polygon is constructed for each edge of the polygon. The X and the Y coordinates of all the four coordinates are obtained from the two vertices, which describe the edge of the roof polygon to which the vertical surface is associated with. The height of the vertical surface is the difference between the roof top elevations and the base elevation as given by the building foot-print.

For example, consider a rooftop polygon with four vertices GDEF as shown in the Figure 4.6. The elevation of the rooftop is obtained along with the building top-print information. The elevation o the building base is obtained from the building foot-print. The height of the rooftop above the ground can be calculated by subtracting the rooftop elevation from the base elevation. For each edge of the polygon GDEF, a rectangular vertical surface is constructed. i.e. For edge GD, a rectangular vertical surface GDCB is constructed, and so on.

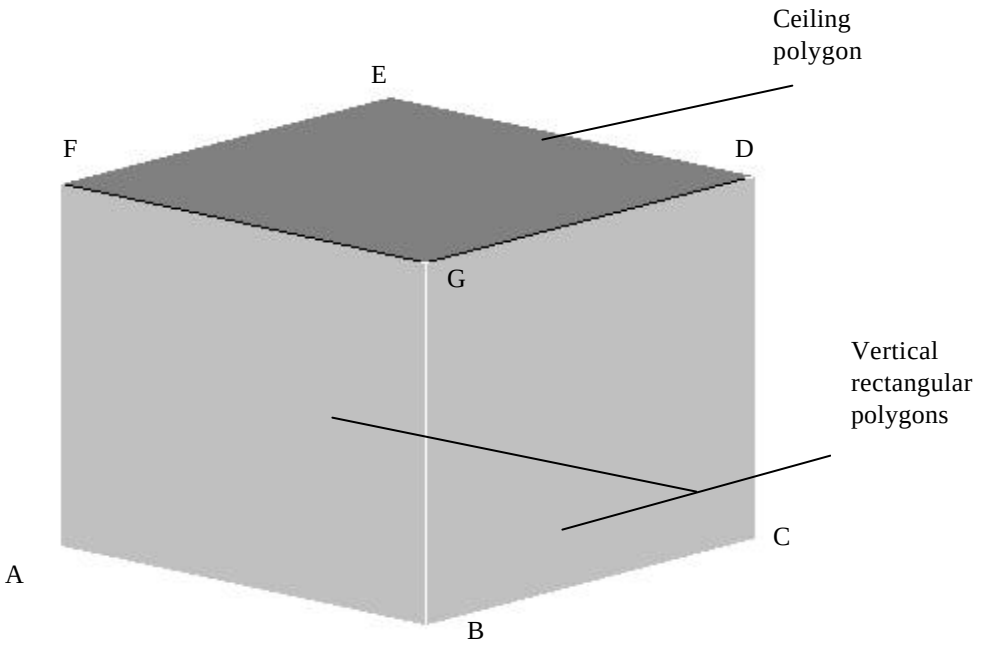

Figure 4.6: Modeling a building with vertical and horizontal polygonal surfaces

A building with different elevations as in Figure 4.4 would have vertical rectangular polygons associated with each edge of all the roof top polygons. All the vertical polygons are considered to have the same elevation for their base. So the building in Figure 4.4 would be represented as a set of vertical and horizontal surfaces as shown in Figure 4.7.

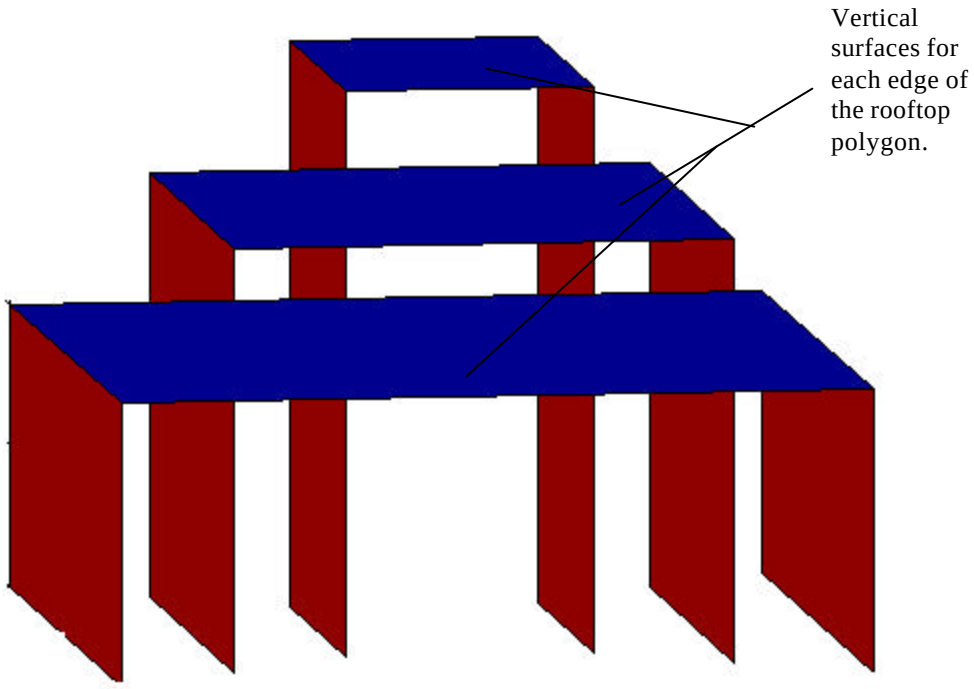

Figure 4.7: Cross-section of a model of a building with different elevations.

Note that such a representation of the building even though incorrectly shows multiple walls, would cause little error while doing propagation prediction outdoors using ray tracing. The ray tracing routine checks only for the first possible intersection of the ray. The penetration along the buildings is generally not considered while modeling the propagation characteristics outdoors. For indoor propagation prediction models use the detailed indoor database while doing prediction. The leakage of signal from outdoors to indoors is modeled as an attenuated transmitted signal from the exterior walls. Once the signal leakage from the outdoor model is obtained to different parts of the building, the detailed indoor model of the building is used to model the propagation inside.

4.4 Building Materials

For deterministic propagation modeling, the information regarding the structure and the placements of the objects is not enough. The characteristics of the surface such as the surface roughness, and the dielectric material properties need to be known to model the environment accurately. However, these details are generally not available and different simplification methods have to be used while modeling the propagation environment. A 6 dB for reflection loss and a 12-dB transmission loss across building walls has been used in a ray tracing based propagation prediction implementation by Schaubach, et. al. [37]. Measurement campaigns conducted in Bristol, UK has proved that a good agreement between the measured power results and ray tracing based results can be obtained for a wall conductivity in the order of 10^{-3} S/m ($s = 10^{-3}$ S/m) and a relative permitivity around 5 (e_r =5) [38].

In the current version of the site-specific propagation prediction tool, the user can either assign a pre-determined attenuation factor for all the surfaces in the environment or specify the attenuation factor for the different surfaces separately. The user can also choose to assign a pre-determined conductivity and relative permitivity for all the walls in the building database. The specified material properties are stored along with the data structure that models the walls of the buildings. These properties are used while calculating the reflection loss and the penetration loss of the surface.

4.5 Combining the Terrain and the Building

In most cases, the data regarding for the terrain and the buildings are available from disparate sources. The terrain data is generally available as a DEM and it is modeled as a TIN using the method as described in the previous chapter. The building data are generally available from independent vendors in the form of building top-prints. The building data has to be overlaid on the terrain data to obtain a comprehensive description of the world.

One of the earliest works in incorporating both the building and the terrain data was performed by Kurner, et. al. [39]. A raster data format is used to model the environment.

The terrain and the buildings were modeled as elevations of a regularly spaced grid. The raster data generally occupies a larger storage area when compared to a vector database. Moreover, the raster data is not flexible enough to represent all the details of an object completely. For example, a raster data representation of the building cannot include the surfaces, which are inside the building and it would be unable to model an indoor-outdoor propagation model-using ray tracing techniques. W.Y.C. Lee suggested a simple propagation method by finding the propagation characteristics of the signal with the terrain data alone and then do with the building data alone. He suggested a method to include both these data to find the signal characteristics with both the terrain and the building. But the method used is simple and is only applicable for LOS [8].

RajGuru, et. al. has proposed a method to overlay the building data on the terrain [23]. According to the method, the triangles in the terrain which overlap with the foot-prints of the building are deleted from the TIN and new triangles are inserted such that the vertices of the building foot-prints. This would mean further computations since the TIN representation has to be updated. Gschwendtner et al [36] have proposed to add an offset to the building heights to account for the terrain variability.

The current implementation uses a method similar to the above-mentioned method. The base of all the vertical surfaces of the building is made equal to the lowest elevation of the terrain. This would make the all the vertical surfaces of the buildings well entrenched into the terrain surface. There would be no error caused by such a simplification in a propagation prediction technique based on ray tracing or any other variant, since only the first surface of intersection would be considered. The ray that gets penetrated through the terrain is generally ignored doing ray tracing.

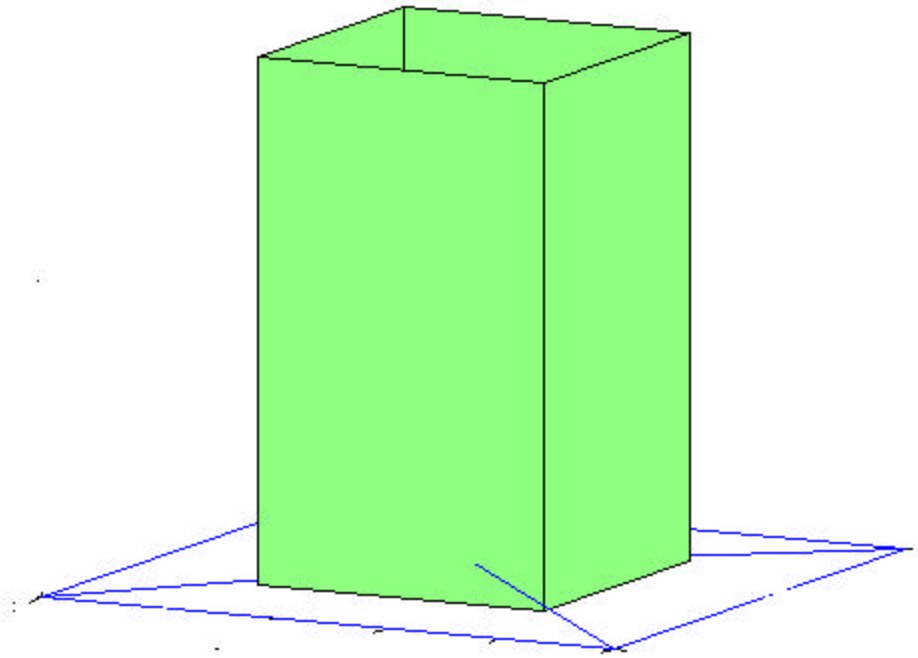

Figure 4.8: The vertical surfaces entrenched into the terrain.

4.6 Resolution required for the Building Database

A high-resolution accurate building database is key for the accurate ray optical based propagation prediction. Studies conducted by G.E. Athanasiadou, et. al. [40], and K. Rizk, et al [38] have found that the predictions are very sensitive to the errors in building corners and building orientations. The building database with a maximum building vertex offset less than 1 meter was found to agree closely with the measured results. So a building resolution of 1 meter is required to obtain accurate predictions.

4.7 Chapter Summary

This chapter describes a method to model the buildings from building top-prints. It also explains a method to overlay the building information on top of the terrain information without causing any considerable impact on the propagation prediction.

Chapter 5

5 Overview of Ray Tracing Techniques

This chapter presents an overview of the ray tracing techniques used for propagation prediction. The first part of the chapter discusses about the motivation behind using a ray tracing based propagation prediction technique. Section 5.2 briefly explains the physics behind ray tracing. The different techniques used for ray tracing are presented in sections 5.3 and 5.4. The complexity of the ray tracing algorithm is discussed in 5.5. Section 5.6 discusses the limitations of propagation prediction using ray tracing.

5.1 Motivation

Wireless system planning and propagation prediction has been an active area of research for the past three decades. Earlier prediction models were based on empirical measurements [41-42]. These models were not site specific in nature and the predictions were primarily based on the distance between the transmitter and the receiver. These empirical models can only be used to predict the narrow band characteristics of the cannel such as the mean signal strength. By the last decade, several researchers such as Bertoni and Walfish [43-44] developed more complicated models, which were used to predict the signal strength more accurately. Some of these models did in fact use site-specific information while predicting the performance of the wireless system. However, all these models were statistical in nature and predicted the signal only within a certain margin of error. These models were only useful in predicting the narrow band characteristics of the channel and did not provide any information regarding the wide band characteristics such as the power delay profile and the angle of arrival information. A more promising approach for predicting the propagation characteristics deterministically was introduced in the early 1990's, using a technique called ray tracing [45] [46].

Ray tracing owes its origin to computer graphics where it is used to render the scenes to synthesize realistic images. Various research conducted by independent researchers have proved that the ray tracing technique could be used to predict the propagation characteristics of a wireless channel [47-50]. The ray tracing technique was found to be more accurate when compared to the earlier empirical models. In addition, the ray tracing model can also be used to predict the wide band characteristics of the channel such as the power delay profile, and the angle of arrival. Propagation prediction using ray tracing is theoretically applicable to a wide variety of environments ranging from dense urban surroundings to indoor maze like scenarios.

The propagation characteristics available from the ray tracing based tool can be used to determine the optimal position of the antenna, the optimal antenna radiation pattern and to find the coverage of a wireless system [51]. With the advances in the field of personal computing over the last decade, the ray tracing technique has become a tool of choice for the wireless engineers to characterize the wireless channel for complex environments.

5.2 Physics of Ray Tracing

The propagation of EM waves along a homogenous medium is governed by the Maxwell's equations. However, the numerical solutions for the Maxwell's equations such as finite element and finite difference method are computationally very intensive and are not feasible for complex real life environment [5]. Therefore, an alternate approach using Geometrical Optics (GO) is generally used to approximate the propagation on characteristics of radio waves in real life environments. Geometric Optics is a high frequency method used for approximating the propagation of Electro Magnetic waves for incident, reflected and refracted fields [52]. The Geometric Optics method assumes that the dissipating energy is radiated in infinitesimally small tubes known as rays and is often referred to as ray optics. To conserve the energy in a tube of rays, the power of the EM waves have to be inversely proportional to the square of the distance that it travels. Ray tracing is a simulation technique, which uses the principles of Geometrical Optics to trace the propagation of EM waves represented as rays.

Geometric Optics was originally developed to analyze the propagation of light at sufficiently high frequencies and hence does not take into account the wave nature of light. It assumes that all that the objects the ray encounters are perfectly smooth and reflects only in the specular direction. Geometrical Optics also fails to account for the energy diffracted into a shadow region when the wave encounters an edge or a corner. At radio frequencies, the diffraction of real EM waves into shadow regions is not negligible and has to be taken into account to model the propagation accurately. A theory known as the Geometrical theory of Diffraction (GTD) was developed by J.B. Keller [53] to supplement GO to model diffraction of the EM waves into shadows. Later on, a more accurate model for diffraction called Uniform Theory of Diffraction (UTD) was introduced by Pathak, et. al. [54]. The GTD/UTD is simple to apply and fits well within the realm of classic ray tracing.

5.3 Ray Tracing Techniques

The ray tracing techniques attempts to find the ray paths between a transmitter and the receiver. The power incident at the receiver due to these different ray paths can be calculated using the free space model [App. A]. The power of the different ray paths when mapped according to the time of arrival of the rays would provide us with the power delay profile of the wireless channel. Two fundamentally different methods are commonly used for finding the ray paths. They are the ‘method of images’ and the ‘Pin-Cushion method’ techniques.

5.3.1 Method of Images

The method of images uses a concept similar to image theory in electromagnetics. The image method starts by constructing an image or a projection of the transmitter in all the building surfaces visible to the transmitter. Then the secondary images of the different primary images are constructed on all the surfaces visible to the primary images. This image mapping of the transmitter is carried on until a chosen maximum numbers of reflections are accounted for. A straight line is drawn from all the images to the receiver.

Finally the valid ray paths are selected from the transmitter to the receiver are selected by drawing a straight line from all the images of the transmitter to the receiver. The path is termed as valid if the straight line from the image to the receiver passes through the actual building surface and not just the image plane.

Fig. 5.1 demonstrates a simple application of the method of images. In Fig. 5.1, the ray from Image 2 to Rx1 is considered valid since it passes through the original building surface, while the ray from Image 2 to Rx2 is not valid since it does not pass through the building surface.

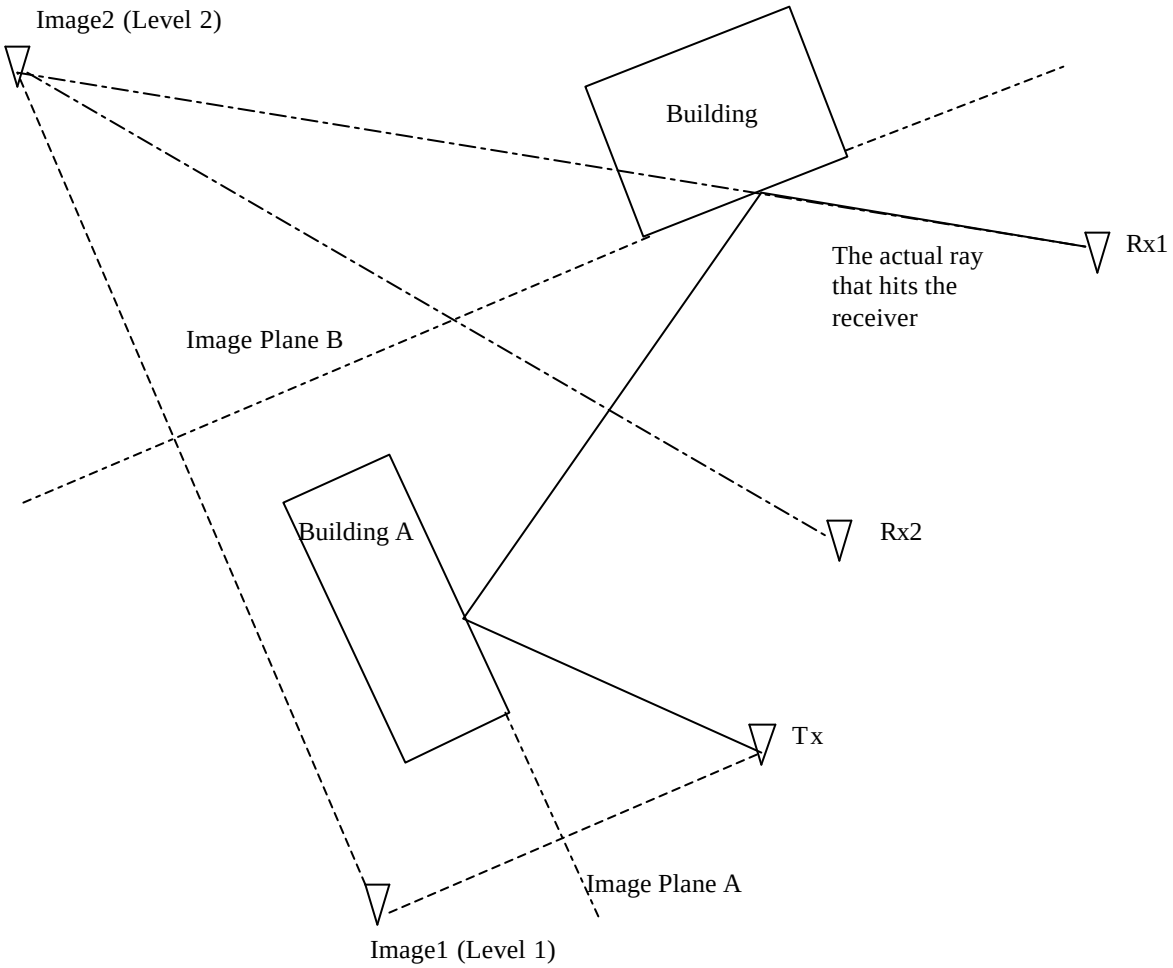

Figure 5.1: Ray Tracing using 'method of images'

The ray tracing technique introduces no kinematic errors and determines exact radiation paths. This technique is successfully used in many wireless prediction tools, which uses two-dimensional ray tracing [50], [55], [56]. This technique when applied to an urban scenario with a 2-D building database assumes that the transmitters and the receivers lie well below the lowest rooftops and the sides of the buildings are flat from top to bottom. The method of images has also been used in indoor scenarios with the reflections from the ceilings and the floors taken into account separately.

The number of images generated using this method grows exponentially with the number of surfaces. Hence the complexity of a ray tracer based on the 'method of images' does not lend itself to complicated 3-D urban scenarios with thousands of surfaces [57], [58].

5.3.2 Pin-Cushion Method

The Pin-Cushion method launches numerous rays from the transmitter into the environment. Each ray is represented as a straight line. The trajectory of each individual ray is followed until it hits a surface. The present ray is then spawned into two. One representing the reflected wave and the other the transmitted wave. The direction of the reflected and the transmitted wave is calculated using Snells' law. Each time the ray hits a surface, the power of the reflected ray and the transmitted ray is calculated by reducing the reflected power loss and the transmitter power loss from the original power of the ray. The reflected and the transmitted rays are then traced until it hits a pre-determined number of surfaces or until the power reduces below a pre-determined level. All the resulting ray segments are checked to see whether it illuminates a receiver. The different ray launching and the receiver modeling techniques are explained in the next section.

5.3.2.1 Ray Launching

To avoid spatial aliasing as much as possible, the rays have to be launched uniformly from the transmitter. In other words, the launch points must be uniformly distributed so that all the regions are equally illuminated using the ray tracing technique. Also, to keep the ray manipulations a minimum, the wave front denoted by the ray should

have identical shape and size. The wave front of each ray can be interpreted as the area of cross section between a ray and its neighbors.

A straightforward method to launch the rays would be to launch the rays from a uniform sphere, by dividing the azimuthal and the elevation angles equally. However, such a division of the spherical surface would have a greater density of the vertices towards the poles and a lesser density of vertices towards the equator. This would mean that there would be more rays emanating from the poles than from the equator (Fig. 5.2).

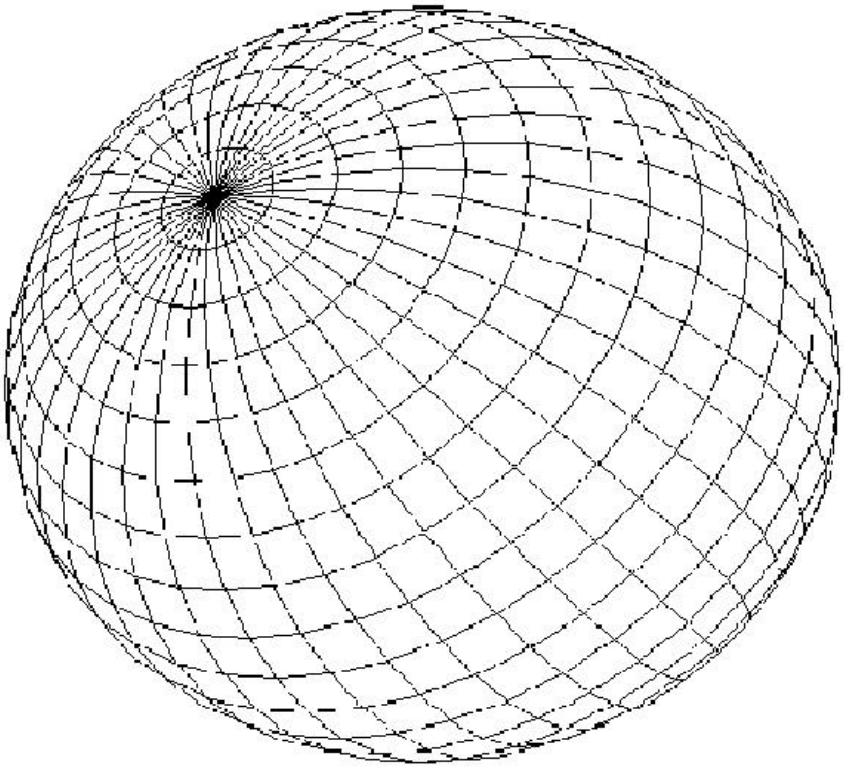

Figure 5.2: A sphere with uniform divisions along the azimuthal and the elevation angles

Therefore, a better technique for launching the rays into a 3-D environment was proposed by [49]. The solution was adapted from the theory of geodesic domes. The vertices of a geodesic sphere provide unbiased launch points and equal angles between the neighbors. The geodesic sphere can be constructed by tessellating the faces of a 20-sided regular polyhedron (icosahedron) and extrapolating the intersection points to the

surface of a sphere. Each icosahedron is subdivided into equilateral triangles along the edge and the vertices of the triangles form the vertices of the geodesic sphere. The rays are modeled as being launched from the vertices of a geodesic sphere.

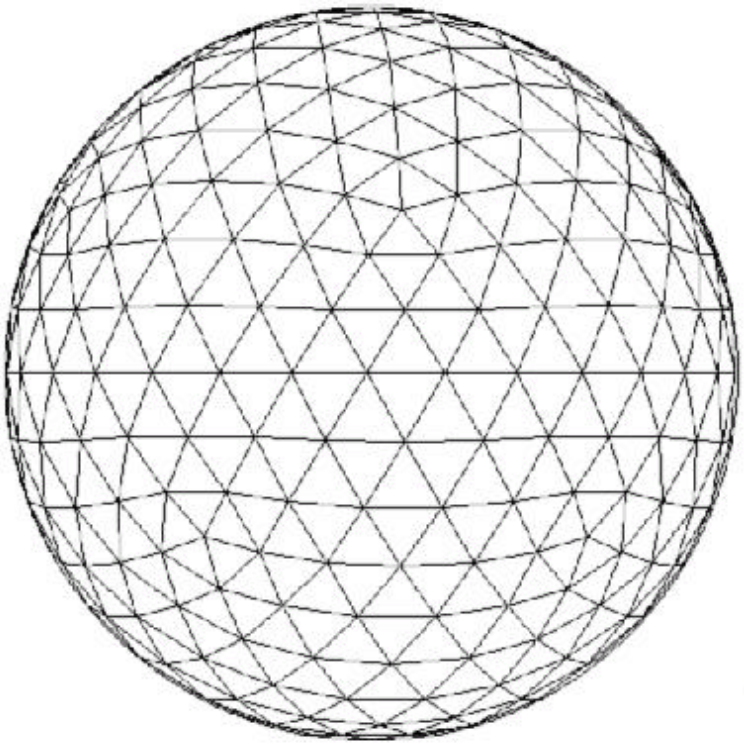

Figure 5.3: The vertices of a Geodesic sphere

5.3.2.2 Modeling the Receiver

The various ray segments of all the rays are checked to see whether they illuminate the receiver or not. The rays that intersect the receiver are analyzed and the power delay profile estimate can be developed by mapping the power of the various rays with respect to the arrival time information of the different rays. However, care must be taken to include one, but only one ray, originating from the transmitter and reflected from the same set of surfaces, will illuminate the receiver. The set of rays originating from the same source and reflected from the same set of surfaces can be considered to be the part of the same wave font. The next section discusses the various methods that are being

employed to model the receiver without counting the rays from the same wave front more than once.

One approach is to model the receiver as a sphere with a finite radius, as determined by the unfolded length of the ray. The receiver is considered to be illuminated by the ray, if the ray hits the reception sphere. Such an approach would work perfectly for a 2-dimensional case. For example, if the rays were transmitted at equal incremental angles d , then the neighboring rays would be Sd distance apart, if the ray has traveled a total distance S from the transmitter. So the receiver can be modeled as having a circular diameter of Sd . This ensures that only one ray from a wave front intersects with the reception sphere [5].

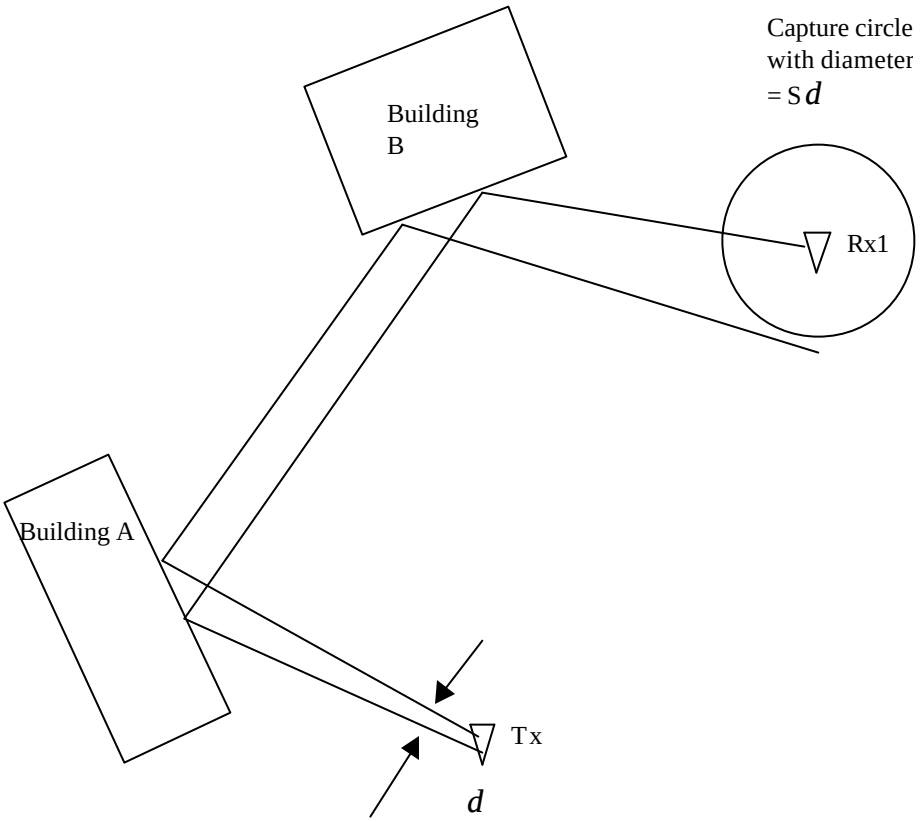

Figure 5.4: 2-D Pin-Cushion method with the capture circle

In the three-dimensional case, the minimum radius for a reception sphere that guarantees that at the least one ray from a wave front will hit the reception sphere is equal to $\frac{1}{\sqrt{3}}$ the distance between the rays. [59],[5]. A sphere with the above mentioned radius would sweep out a circular area across the wave front. However since the transmitter emits the rays along the vertices of a geodesic sphere, there is always a probability that the more than a single ray from the same wave front would fall within the reception sphere (Fig. 5.5). This causes ‘double counting’ of the rays, and could incorrectly indicate that a higher power is incident on the receiver.

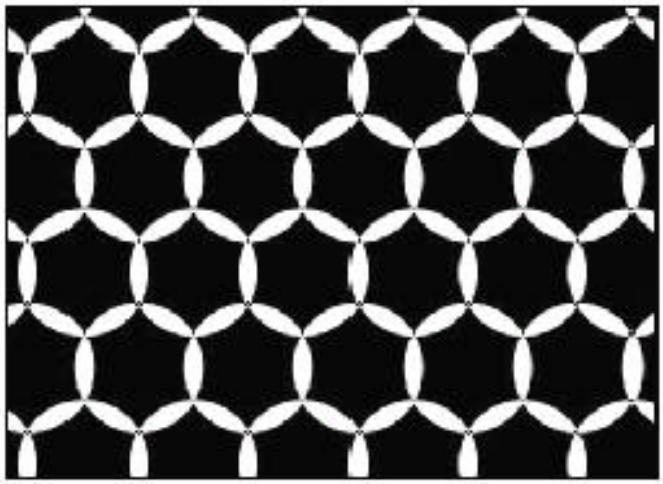

Figure 5.5: Double Count Errors (white regions) along an ideal geodesic wave front (source: Reference 23).

A distributed wave front approach may be used to solve the 'double counting' problem. According to the distributed wave front approach, when a ray hits the reception sphere, it is not counted as a hit or a miss. Rather, each ray, which hits the reception sphere, is given a certain weighting, which is inversely proportional to the distance from the center of the reception sphere [60]. A weighting function has been developed so that the error due to double counting is minimal. The weighting function does not have an analytical expression and is solved using numerical methods and has been tabulated for the different distances between the point of intersection and the center of the reception sphere. The rays that hits the reception sphere are then multiplied by a value determined by the weighting function and the distance between the point of intersection and the center of the sphere. The weighting function is adjusted so that the if the receiver point is precisely intersected with a ray (zero distance) it accumulates 100% of the energy and if it is being hit by a neighboring ray it would accumulate 0% of the energy of the ray. This method ensures that the errors due to double counting are avoided. The distributed wave front model is proven to give results that agree closer to the measured power levels than the hit and miss method [60].

5.4 Generalized Ray Tracing

In the usual Pin –Cushion method, the rays are modeled as straight lines. Though, the simple representation of the ray makes it easier to implement intersection tests, such a technique can cause spatial aliasing and does not allow to exploit the coherence of the rays. Researchers have devised several methods for modeling the rays, which exploit the coherence of the rays. These methods instead of operating on individual rays operate simultaneously on entire families of rays bundled as beams or cones or tubes of rays [66]. Most of these techniques owe its origin from the field of computer graphics.

5.4.1 Tube Tracing

Tube tracing, instead of tracing individual rays, tracks the path of a group of adjacent rays often termed as ray tubes. In most cases, for the sake of simplicity, the ray tubes are modeled as having a triangular cross section associated with them (Fig. 5.6). Each ray tube is tracked by simultaneously tracing all the individual rays that define the cross section of the ray tube. The ray tubes uses the same technique as the Pin-Cushion method to trace the individual rays that define the cross section of the ray tube. Receivers are modeled as points in space and a receiver is considered to be illuminated by the ray tube if the receiver is contained in the ray tube cross section of the ray tube.

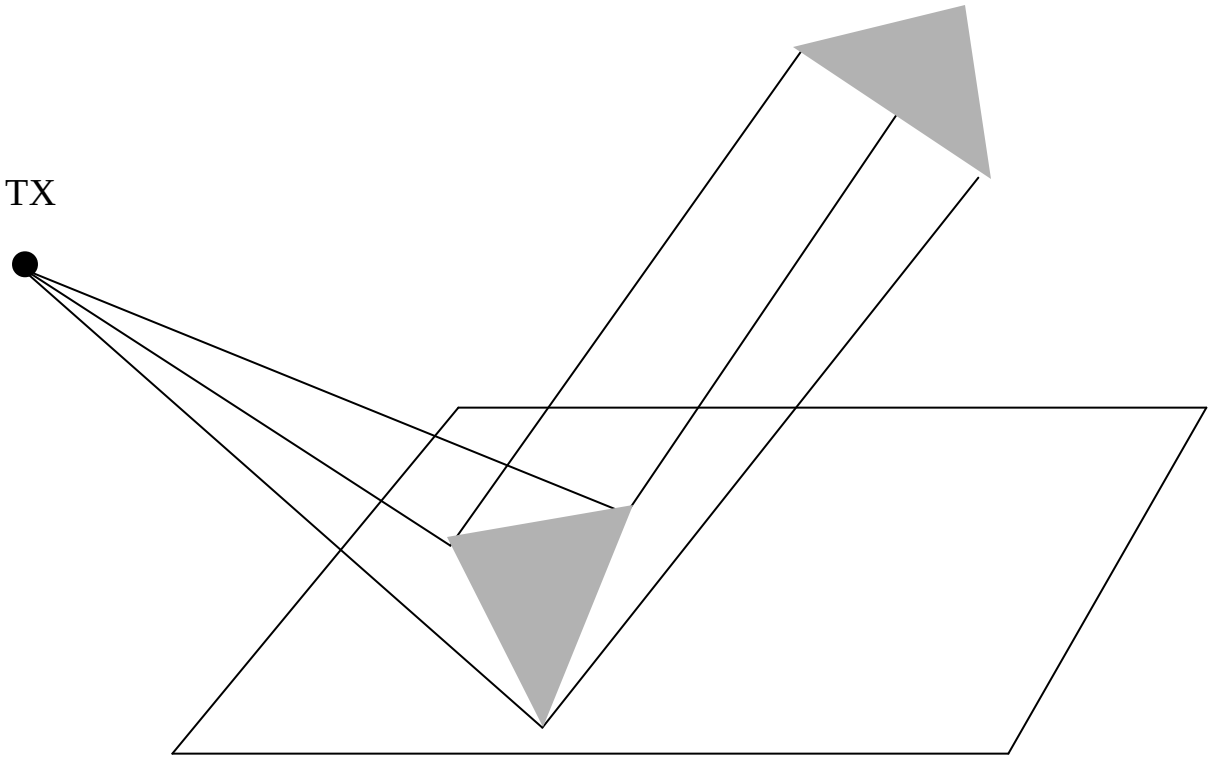

Figure 5.6: Tube tracing

Unlike the Pin-Cushion method, the tube tracing technique can easily be adapted to environments which has curved surfaces in it and is widely used for radar applications [60]. However, the computational complexity of the tube-tracing algorithm is generally higher than the Pin-Cushion method since all the rays that encloses the ray tube has to be tracked. Many researchers have used tube tracing successfully for three dimensional wireless propagation predictions [61][62].

5.4.2 Beam Tracing

Beam tracing, a generalization of the method of images, was originally proposed by P. Heckbert and P.Hanrahan [63] as a rendering technique for image synthesis applications. The Beam tracing technique replaces the ray with beams that are represented as cones with polygonal cross sections. The beam consists of a collection of

rays originating from a transmitter (or an image of the transmitter) and reflected or transmitted from a planar polygon.

The Beam tracing algorithm assumes that all the surfaces in the environment are represented as planar polygons. The beams are tested for intersection with the various surface elements in the environment. The polygons that represent the environment are first sorted according to the distance from the beam. The beam intersection tests are carried out with the nearest polygon first. An image of the transmitter is first computed by reflecting the transmitter through the plane of the polygon. A new beam is created with the image of the transmitter as its apex and the planar cross section of the reflective surface as its polygonal cross section. Unlike the rays, which either hits or misses a surface, the beams can be partially occluded from hitting a surface. If the beam is partially occluded from hitting a surface, the cross section of the beam is sub divided into different beams using polygonal clipping techniques. The cross section of the beam hit by the surface is reflected from the surface (Fig. 5.7a and Fig. 5.7b). The polygonal cross section(s), which represents the part of the beam that misses the surface, undergoes further beam surface intersection tests. Due to the sorting involved in the beam surface intersection tests, the complexity of a beam tracing is in the order of O (n^2).

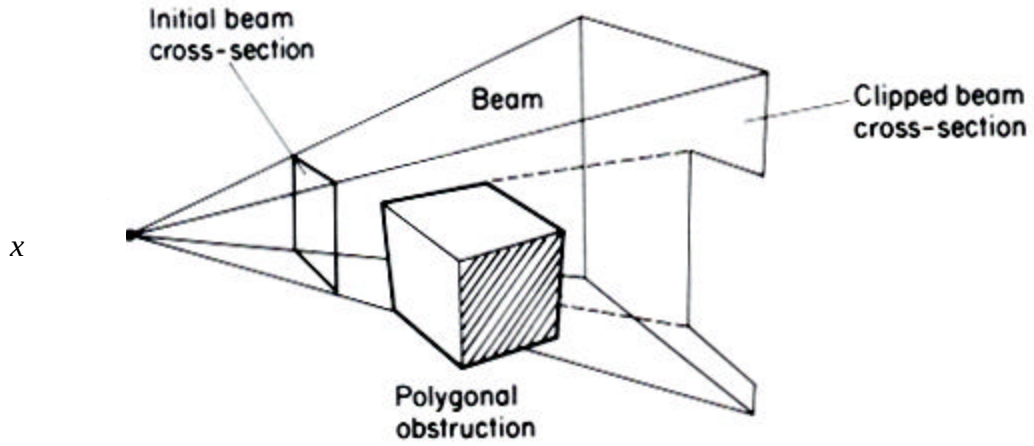

Figure 5.7a: The beam intersected with a polygonal surface and the clipping of the beam

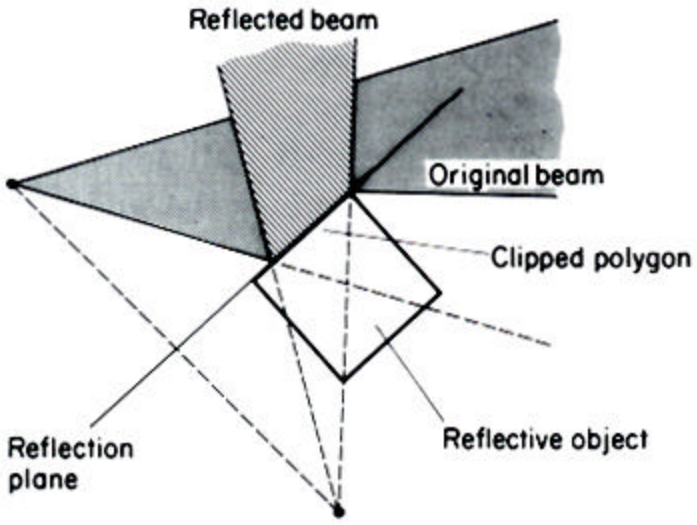

Figure 5.7b: The top view of Fig. 5. 7a with the image of the transmitter (Source: Reference 29)

Propagation prediction using beam tracing techniques was found to be computationally more efficient than standard ray tracing while modeling propagation with only one or two reflections [64]. However, as the number of reflections increases, the beam splitting and the sorting of polygons was found to take a heavy toll on the computational efficiency of the beam tracer.

5.4.3 Vertical Plane Launch Technique (VPL)

The Vertical Plane Launch technique was introduced by H. Bertoni and G. Liang to predict the propagation characteristics in an urban environment [65]. The VPL method relies on the fact that almost all the walls of the buildings are vertical and hence all the rays, specularly reflected and diffracted from vertical edges would follow the same slope in the vertical plane. This method accounts for specular reflections from vertical surfaces and diffraction from vertical edges but only approximates diffraction from horizontal edges (rooftops).

According to the VPL method, the base station antenna launches a series of vertical planes represented as 2-D rays. A standard 2-D Pin-Cushion method is used to trace the vertical planes. However, unlike the standard 2-D ray tracing method, the 2-D rays are also allowed to transmit through the building walls. This represents the part of the vertical plane that has transmitted over the building. The diffraction due to vertical edges is approximated using a number of vertical planes launched from the vertical edge. The VPL method assumes that the rays diffracted from the horizontal edges (rooftops) also lie in the same vertical plane. This would distort the subsequent ray paths. However, the distortion is small when the horizontal corner is close to being perpendicular to the vertical plane containing the incident ray or the slope of the incident and diffracted rays are small.

The receiver modeled as a 2-D sphere (circle) as described in the pincushion method. At the receiver, the vertical ray profile of the rays is found by examining the profile of all the buildings in the unfolded set of vertical plane segments between the source and the receiver [65]. The vertical trajectory of the rays is found analytically, thereby giving the ray paths in three-dimensions. Figure 5.8a explains the 2-D Pin-Cushion ray tracing and Fig. 5.8b represents the 3-D view of the ray tracing performed.

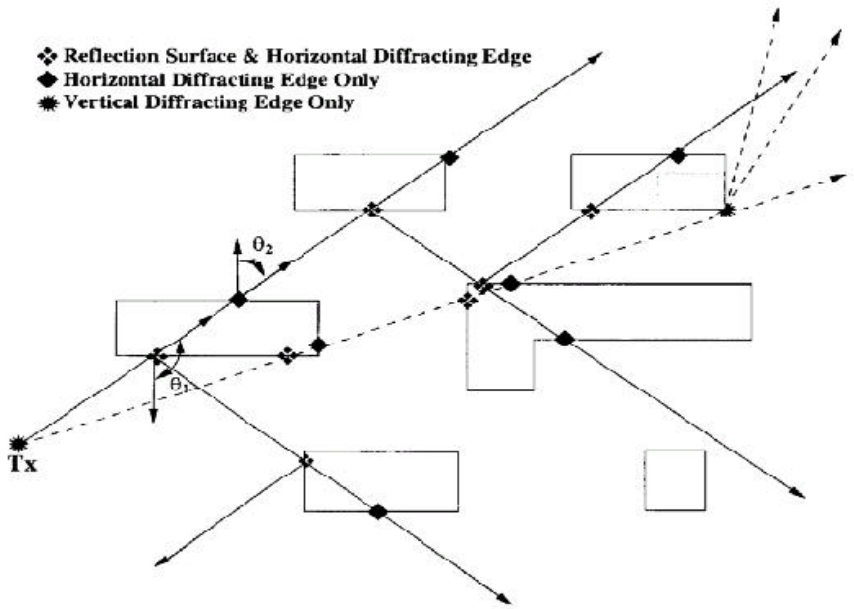

Figure 5.8a: The 2-D representation of the Vertical Plane launch method

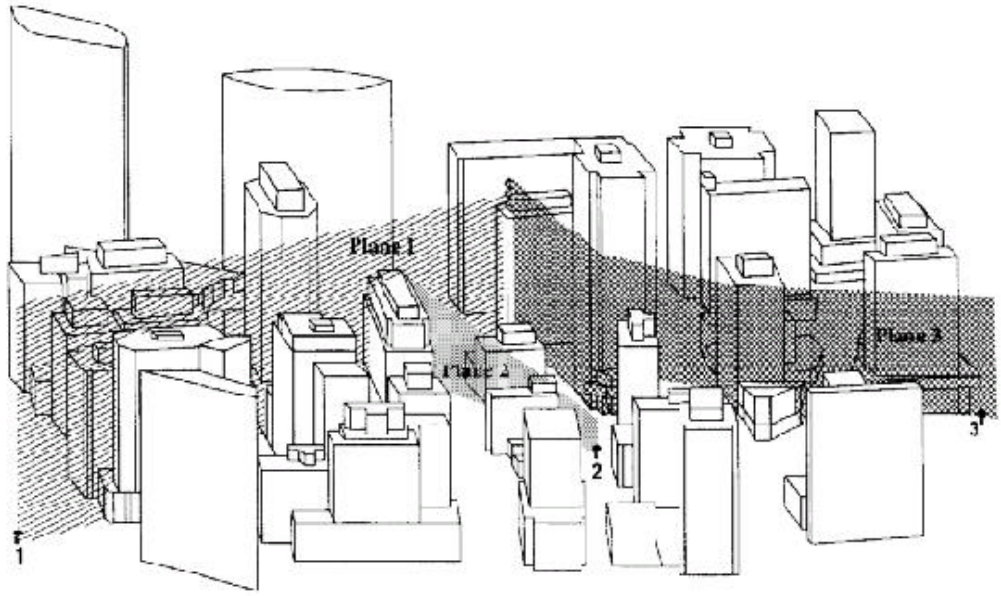

Figure 5.8b: The 3-D ray tracing method using the VPL method (Source: Reference 28).

The VPL method, was found to be computationally less complex when compared to a full 3-D ray trace. Measurements done at Rosslyn, Virginia, showed that a prediction accuracy of upto a few decibels was possible using the VPL method [5].

5.5 Complexity of the Ray Tracer

Consider an environment with K surfaces, which are distributed, in a random fashion. Let the maximum number of reflections considered for each ray be equal to n. In the worst case scenario, each ray has to undergo K^n intersection tests. So the total number of intersections required is equal NK^n, where N is the total number of rays emitted by the transmitter. The above mentioned calculation assumes that each ray is tested for intersection with every surface in the environment.

5.6 Limitations of Ray Tracing

Ray Tracing is not a cure for all the problems in propagation prediction. The ray tracing technique has its own limitations. Ray tracing as described earlier considers only specular rays as reflected from the surfaces. In other words, this means that the rays that hit the surface are only reflected in the direction as determined by the Snell's law. This is hardly true. The Electro Magnetic wave that hits a surface scatters the energy in all directions, whose power is determined by the frequency of the EM waves and the surface roughness of the surface under consideration. Even, though this phenomenon can be modeled by spawning many numbers of rays each time the ray hits a surface, this would increase the computational complexity of the ray tracer manifold.

Yet another problem while using ray tracing is 'spatial aliasing' [66]. Spatial aliasing arises is due to the fact that only a finite number of rays can be modeled in a computer. The discrete rays can always miss a genuine surface while checking for intersection. One of the methods used to mitigate any spatial aliasing is to send a large number of rays. This can only reduce the problem but not solve the problem as such .

Even though in principle ray tracing can predict the fast fading characteristics of the channel, this is not the case. In practice, the building data base position accuracy for a real environment is often less than 0.5 m This is an order or so higher than the wavelength of the EM waves under consideration. This causes errors in predicting the phase of the rays when they reach the receiver. So the interference pattern of the multipath waves cannot be replicated exactly. Moreover, the intersection of the waves with different surfaces would cause a phase shift in the waves depending on the surface roughness and the material used. It is not practically possible rays with such fine details. But nevertheless, ray tracing can be used to find the pattern of the Power delay profiles at the receiver, though with a certain phase error. The angle of arrival of the EM waves can also be predicted to a certain degree of accuracy.

5.7 Conclusion

This chapter presents the different ray tracing techniques used for site specific propagation prediction. The physics behind ray tracing is explained. The complexity of the ray tracer and the limitations of a ray tracing based approach are discussed in detail. Although recently new techniques based on finite element analysis have been proposed, ray tracing still remains the number one choice for predicting the propagation of radio waves.

Chapter 6
6 A Novel Prediction Technique for Broadcast Channels

This chapter presents a novel method to predict the propagation characteristics of multiple points in space. This method promises to significantly reduce the computation time when compared to the standard 3-D Pin-Cushion based ray tracing algorithm.

6.1 Introduction

The previous chapter explained the different techniques that can be used to predict the propagation characteristics at a particular point in space. All the different techniques described are well suited for predicting the propagation characteristics of a point to point network. The receivers and the transmitters are modeled as points in space and the propagation characteristics of the receiver at a particular position is predicted using ray tracing algorithms. Consider a broadcast system, such as a Cellular system or a Wireless LAN system. The base station antennas of such systems are placed so that a maximum coverage can be obtained over a particular region. Hence the system design engineer would be interested in knowing the propagation characteristics of multiple positions in space rather than just a single point in space.

Many commercial propagation prediction tools such as SitePlanner and Winprop use ‘grid mode predictions’, where the propagation characteristics of a uniformly spaced horizontal grid of receivers are predicted. The grid mode predictions would help the wireless engineer to visualize the propagation characteristics of a particular region in space. The algorithms used to optimize the placement of the antenna [67] [68] [69] also require grid mode predictions as their input.

While using the traditional ray tracing approach, multiple receivers have to be modeled at uniformly spaced interval to find the ‘grid mode’ propagation characteristics of a wireless system. This would mean that intersection tests must be performed for each of the receiver points. This can be computationally expensive especially when there are a large number of receivers. An algorithm for finding the propagation characteristics from

a transmitter to multiple receivers using the 3-D image method was presented by O'Brien, et. al. [70]. However, an image-based approach limits the scope of the prediction technique to less complex environments. This chapter presents a novel propagation prediction technique based on a 3-D tube tracing method for grid mode predictions.

The first part of the chapter explains the kinematics of tube tracing. Section 6.3 explains the new grid mode algorithm in detail. The computational complexity of the new algorithm is compared with standard ray tracing technique in Section 6.4. The new algorithm is compared with the standard ray tracing algorithm in terms of its accuracy and computation time.

6.2 Tube Tracing

Tube tracing, as explained in the previous chapter, traces tubes of rays instead of individual rays. For the algorithm under consideration, the ray tube is assumed to have a triangular cross section. A triangular cross section is chosen owing to its simplicity in representation and ease of tracking the ray tubes. The transmitter launches numerous ray tubes into a numerical environment. Each ray tube is traced by tracing the three rays, which define the triangular cross section of the ray tube. A ray tube is considered as being intersected by a surface if all the three rays that enclose the ray tube are intersected by the same surface. If all the three rays are not intersected by the same surface, the ray tube is assumed to be intersected by an edge of a surface and is not counted as a valid intersection. In such cases, the ray tube is terminated (Fig. 6.1).

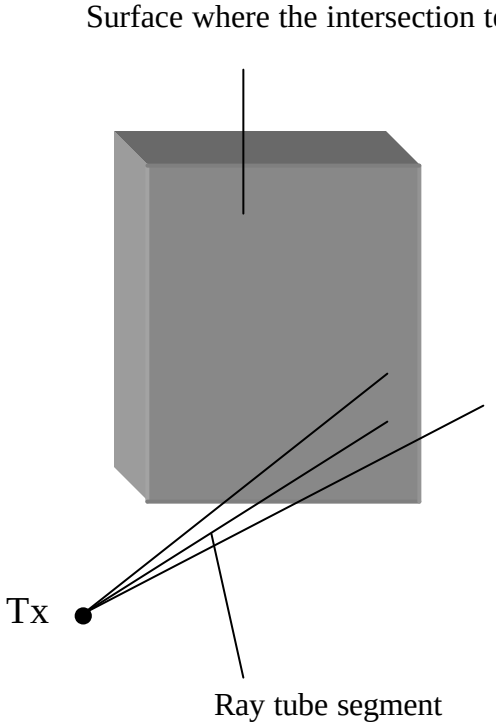

Figure 6.1: The ray tube intersected by an edge of a surface

The intersection of the ray tube with a surface creates a triangular region that can be considered as being illuminated by the ray tube. The part of the ray tube between the transmitter and a surface or between two surfaces is called a ray tube segment. Each ray, which defines the cross section of the ray tube, is then reflected from the surface of intersection in a direction determined by Snell's law. The ray tube is further tested for intersection with the other surfaces in the environment until a fixed number of reflections, as defined by the user, are considered (Fig. 6.2).

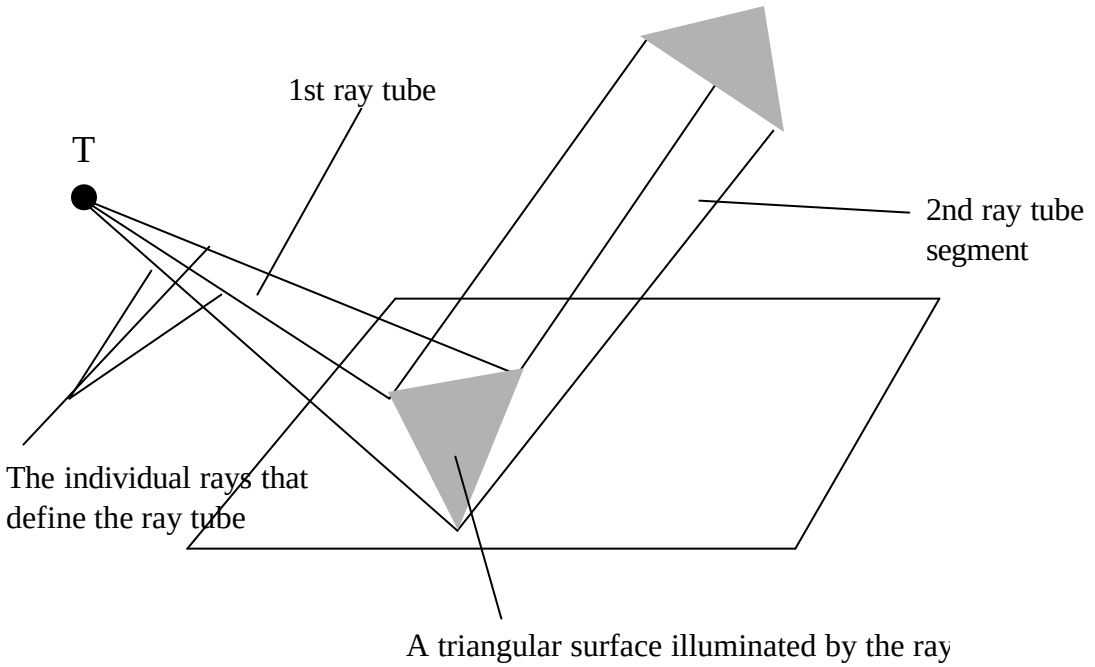

Figure 6.2: The ray tube tracing

A receiver is considered to be illuminated by the ray tube segment, if the receiver is inside the triangular cross section that defines the ray tube.

6.3 A Novel Grid Mode Prediction Algorithm

The proposed grid mode prediction algorithm predicts the signal characteristics of multiple receivers, which are uniformly spaced at a constant elevation from the ground. As in the standard ray tracing algorithm, the grid mode algorithm uses the concept of finding all the ray paths between the transmitter and the receiver for predicting the propagation characteristics at a point. The grid mode algorithm uses tube tracing to find all the possible paths between the transmitter and the receivers. The environment need to be modeled as a set of planar polygons and represented in the vector format. The transmitter is modeled as a point source that emits ray tubes into the environment. However, the receivers are not modeled as point objects. The grid mode prediction algorithm assumes that all the receivers are uniformly placed in a horizontal grid. The grid of receiver points can be thought as being embedded in a ‘virtual’ flat surface. Let

this surface be called the ‘receiver surface’. The next section explains how the ray paths from the transmitter to the multiple receivers are traced.

The transmitter emits numerous ray tubes into the environment. As explained in the previous section, the ray tubes are tested for intersection with all the ‘real’ surfaces in the environment. The intersection of the ray tube with a surface results in a ray tube segment as shown in Fig. 6.2. The ray tube segments are reflected back from the surfaces and is tested for intersection with the other surfaces in the environment until a user defined maximum number of reflections are taken into account. All the individual ray tube segments are tested for intersection with the ‘receiver surface’. If there is an intersection with the ‘receiver surface’, the points of the intersection are computed. These points of intersection constitute a triangular region in the ‘receiver surface’. However, unlike the actual surfaces, intersection with the ‘receiver surface’ does not cause any change in the trajectory or the power of the ray tube segment (Fig. 6.3).

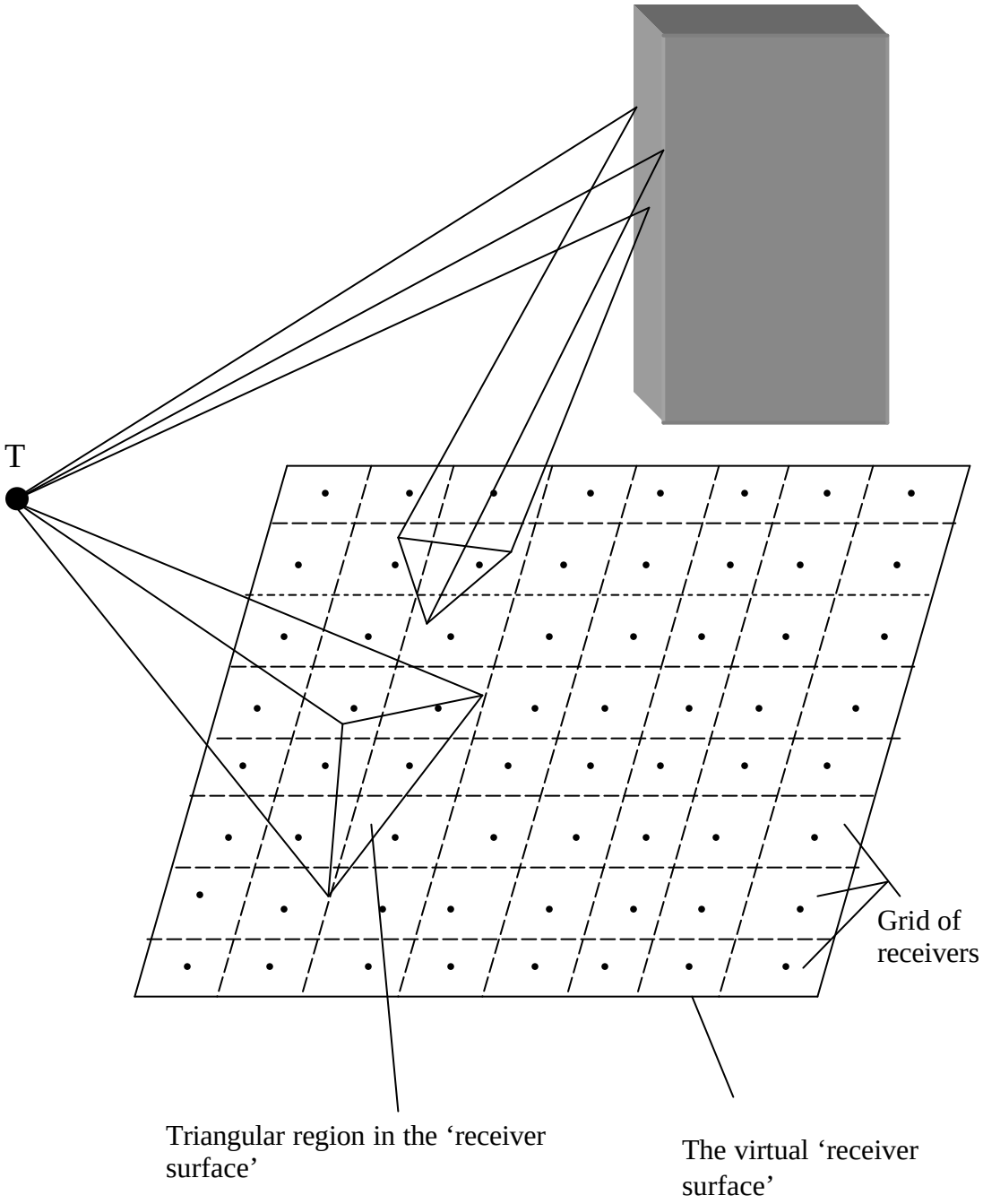

Figure 6.3: The ray tube segment intersects with the virtual ‘receiver surface’

Any receiver location inside the triangular region can be considered as being illuminated by the ray tube segment. The grid of receivers need to be checked if they are being illuminated by the ray tube segment. One method to do this is to check for all the receiver locations along the grid. This might be computationally very expensive,

especially if the number of receivers in the grid is very high. An alternate simpler approach is described next.

The maximum and the minimum x and y points of the triangular region is computed. A rectangular sub-grid, which encloses the maximum and minimum x and y coordinates, is formed (Fig. 6.4). Only the receivers in the sub-grid need to be checked whether it is inside the triangular region or not. The grid locations, which are outside the sub-grid, would not be inside the triangular region and need not be considered.

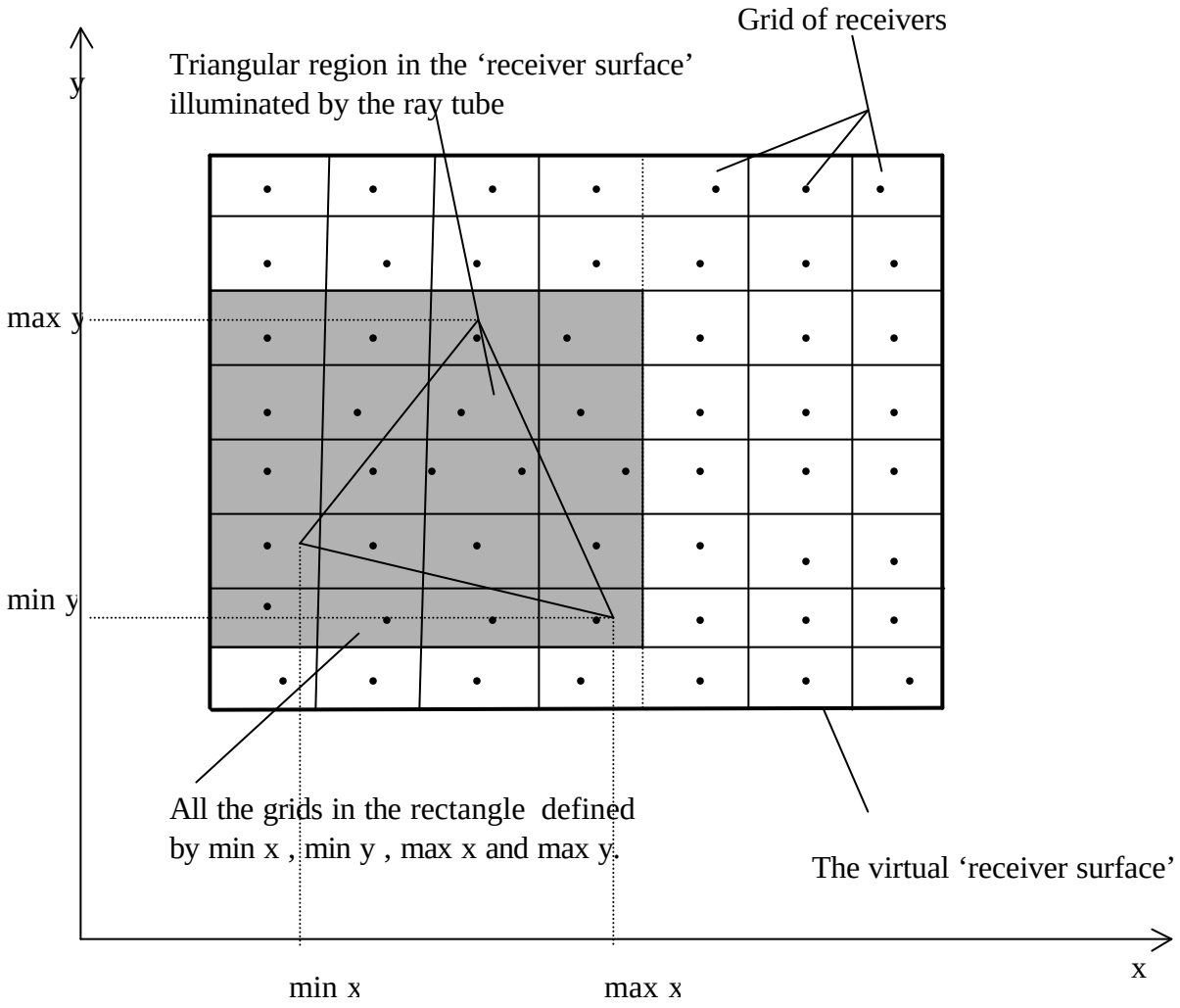

Figure 6. 4: The sub-grid of receivers that has to be checked for illumination

All the receiver grid locations inside the triangular surface are considered to be illuminated by the ray tube segment. The total distance that the ray tube has traveled from the transmitter is computed. The power due to the ray tube segment can be calculated by using the free space model. The power delay profile of all the receivers can be obtained by mapping the power obtained at each receiver with respect to the time of arrival of the ray tubes.

6.4 Computational Complexity

In this section, the total number of intersection tests required for a grid mode technique is compared with the standard 3-D ray tracing technique.

6.4.1 Standard Ray Tracing

Let the total number of receivers to be modeled be equal to r. Let a total of N rays be emitted from the transmitter into an environment with k polygonal surfaces. A maximum of n reflections is considered. Then the total number of intersection tests to be considered (worst case scenario) is equal to $N((k+r)^n)$.

6.4.2 Grid Mode Algorithm

Let the number of receiver surface to be considered is equal to 1. With the same parameters as used for the standard ray tracing algorithm, the number of ray tube intersection test is equal to $N((k+1)^n)$

Note that the ray tube intersection involves more computation when compared to the standard ray tracing intersection tests, since the intersections of all the three ray segments have to be taken into account. The intersection tests of the ray tube segment can be roughly taken as being three times more complex than the standard ray intersection tests. So the complexity is equal to $3N((k+1)^n)$.

An example to compare the computational complexity of the new grid mode prediction algorithm with the standard ray tracing algorithm numerically is given below. Consider a 1-sq. Km of area where a wireless system has to be installed. Let the propagation characteristics at every 1m need to be estimated. Using the standard ray tracing algorithm, the total number of receivers to be modeled is equal to 10^6. Let the total number of surfaces in the environment be 100 and only a maximum of two

reflections be taken into account. In the worst case scenario, intersection tests need to be performed for all the receivers for each of the ray segments. In the standard 3-D ray tracing technique, the total number of intersection tests for each ray, is approximately equal to $(10^6)^2$ where n is the number of reflections to be taken into account. With the new grid mode prediction algorithm, for each ray tube, the number of intersections to be taken into account for each ray tube is equal to $3(101)^2$. Thus the grid mode algorithm would significantly reduce the computation time for a grid mode prediction.

6.5 Experimental Results

The grid mode prediction is tested in a rectangular box with a dimension of 100m x 100m x 50m as shown in Figure 6.7. The transmitter is placed in the center of the cubic box 10m above the ground level. The transmitter and the receiver antennas are isotropic. The wavelength of the EM waves emitted from the transmitter is assumed to be 1m (Frequency = 300 MHz). Let the power of the transmitter be equal to 1 Watts. All the walls are considered to be purely reflective with no reflective loss associated with it.

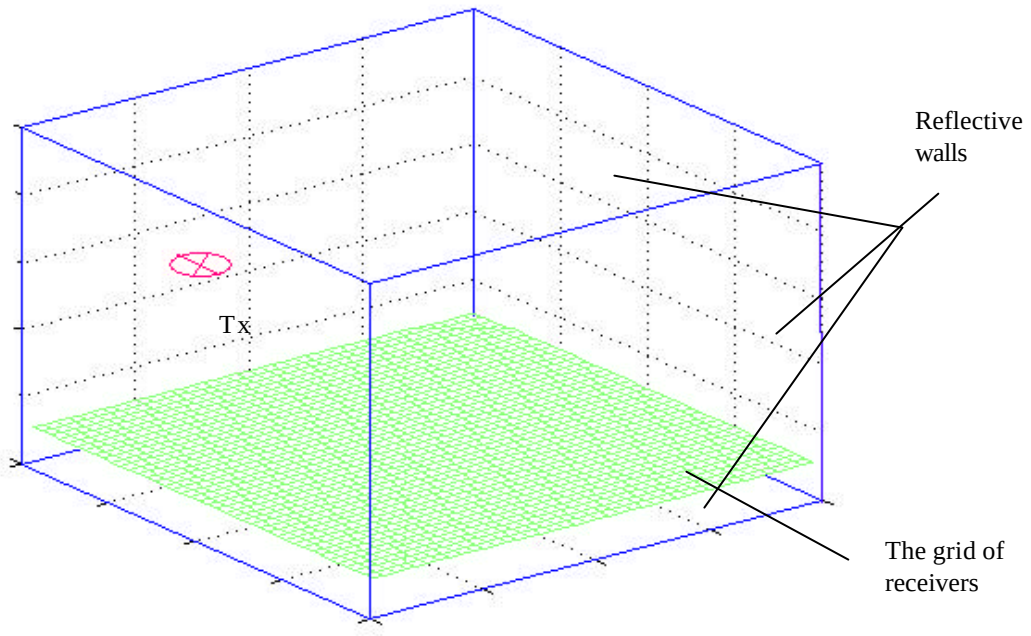

Figure 6. 7: The Environment where the experiments are carried out

6.5.1 Accuracy Test

The algorithm is tested with 100 receivers uniformly spaced at an elevation equal to 1cm above the ground. Figure 6.8 shows the mean signal strength obtained using standard 3-D ray tracing algorithm. Only a maximum of one reflection from the walls is taken into account. The total number of rays considered for simulation is equal to 100,000.

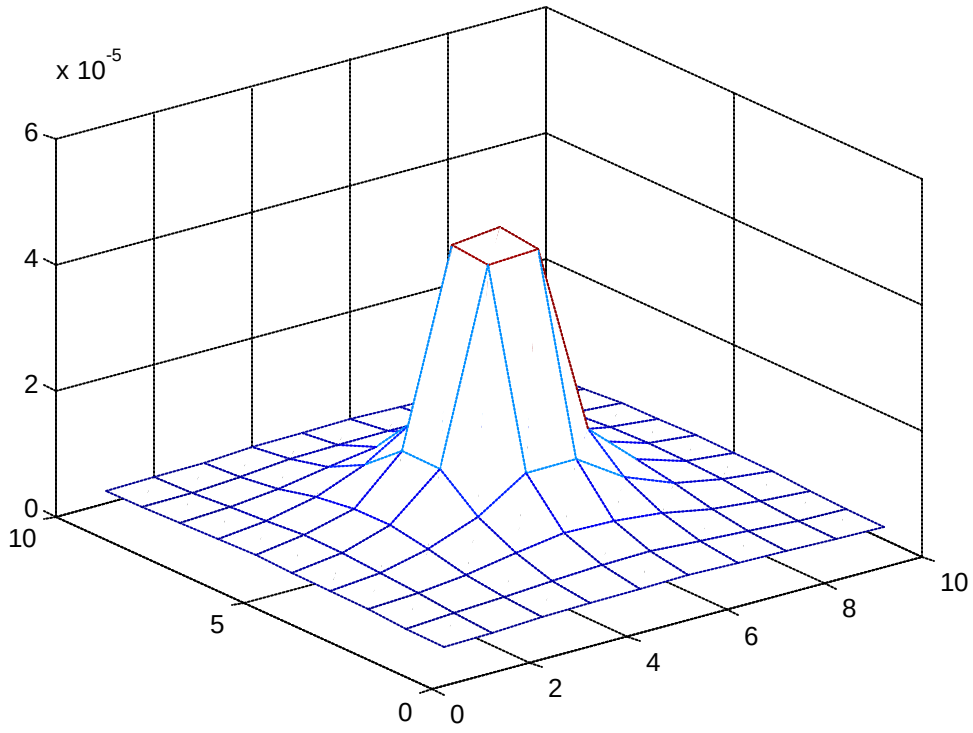

Figure 6.8: The mean signal strength obtained at multiple receivers using 3-D ray tracing

The grid mode algorithm is tested with the same experimental set up. A rectangular 'receiver surface' with a grid spacing of 10mx10m is considered at an elevation of 1m above the ground. The number of ray tubes emitted is equal to 100,000. Figure 6.9 shows the mean signal strength as obtained by the new grid mode prediction algorithm.

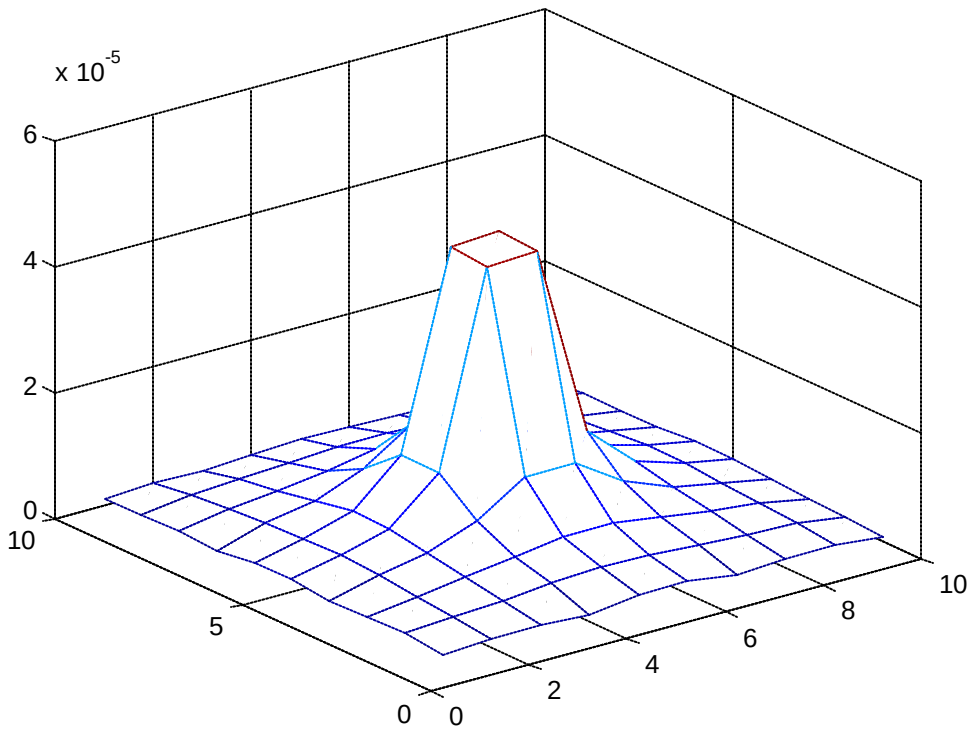

Figure 6.9: The mean signal strength obtained using the new algorithm

Figure 6.10 shows the difference between the mean signal strength as obtained from the ray tracing algorithm and the grid mode prediction algorithm.

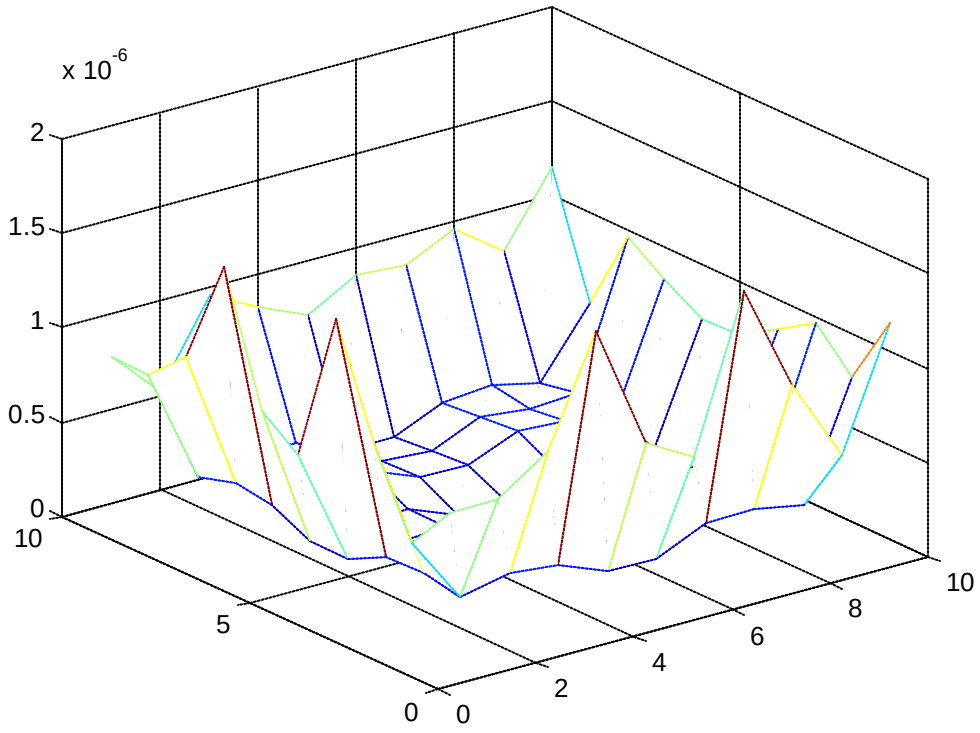

Figure 6.10: The difference between the mean signal strength between the grid mode prediction and standard ray tracing

The grid mode predictions were found to give almost the same results as the standard ray tracing algorithms. A significant difference between the prediction results was found only towards the reflective walls. This is due to the fact that the ray tubes are considered invalid when it hits more than one surface. The mean square difference between the two predictions was found to be equal to 3×10^{-13} W, where as predicted signal strengths were in the order of 10^{-6} Watts.

The grid mode prediction algorithm is now compared with standard 3-D ray tracing method in terms of its computational speed.

6.5.2 Experiment 1

This experiment compares the computational speed of the two algorithms by varying the number of receivers in the experimental set up. The environment under consideration is the same as described in the previous section. This experiment is carried with the transmitter emitting 100,000 rays or ray tubes. Only one reflection is taken into account while predicting the power delay profile. All the receivers are considered to be uniformly distributed at an elevation 1cm. above the floor level.

Number of receiver points	Computation time (in sec) Ray tracing	Computation time in sec Grid Mode prediction
10	10	93
100	45	93
1600	644	92
10000	3776	93

Table 6.1: Comparing the 3-D ray tracing algorithm with grid mode algorithm in terms of computational speed by varying the number of receiver points

As the number of receiver points increases the computation time of the Standard Ray tracing algorithm was seen to be increasing linearly. In the grid mode predictions, there was more or less no change in the computation time as the number of grids in the grid mode prediction increases. The grid mode prediction method has a significant advantage over the standard ray tracing algorithm especially as the number of receiver points increases.

6.5.3 Experiment 2

The computational speed of the two algorithms is compared by varying the maximum number of reflections considered while predicting the propagation characteristics. The environment in which the experiment is conducted is the same as described in the previous two experiments. The number of receiver points considered is

equal to 1600. The receivers are considered to be placed uniformly over a horizontal grid at 1m above the ground.

Number of reflections	Computation time (in sec) 3-D Ray tracing	Computation time in sec Grid mode prediction
0	320	8
1	644	92
2	2122	114
3	4403	186

Table 6.2: Comparing the 3-D ray tracing algorithm with grid mode algorithm in terms of computational speed by varying the number of reflections considered

As the number of maximum reflections taken into account increases, the computational speed of the grid mode predictions far outweigh the standard ray tracing algorithm.

6.6 Conclusion

This chapter introduces a new algorithm for predicting the performance of a grid of receivers. The propagation predictions of the new algorithm matches closely with that of the standard 3-D Pin-Cushion method. The new grid mode algorithm was compared with the standard 3-D Pin-Cushion method in terms of its computational speed and was found to significantly reduce the computation time for predicting the propagation characteristics of multiple receivers.

Chapter 7
7 Conclusion

This thesis presented a collection of previous and new research in the various aspects of a ray tracing based site-specific propagation prediction. The first part of the thesis concentrated on modeling and the representation of the environment for a ray tracing based propagation prediction. The latter half focused on the techniques used for predicting the propagation of a wireless channel.

7.1 Summary of Work

A ray tracing based propagation prediction technique requires that all physical objects in the environment be modeled accurately. Chapter 2 provided a survey of the different geographic products currently available that can be used to model the environment for a ray tracing based application. The different geographic products such as DEMs, building top-prints and building foot-prints were introduced and their availability and the resolution were discussed.

Chapter 3 concentrated on the different aspects related to the modeling of the terrain. It was concluded that the terrain is best represented as a Triangular Irregular Network (TIN), for a ray based propagation prediction technique. The TINs represent the terrain as an irregular network of triangular surfaces in a vector format. However, the TINs are not readily available and it must be developed from common terrain Digital Elevation Models or DEMs. The different methods of converting a DEM into a TIN were evaluated in terms of its computational speed and the total number of surfaces. It was found that a Delaunay-based triangulation algorithm is most suitable for a ray tracing based application(s), since it requires only a minimum number of triangular surfaces to represent a terrain. Additionally this method allows direct control of the maximum error produced in the transition.

Chapter 4 presented an original technique, which may be used to model the buildings from the building top-print information. With this method, the buildings are represented as a set of horizontal and vertical flat polygonal surfaces. A novel method to combine the building information with the terrain data was presented and it was shown that this method is computationally less intensive than the previously suggested methods.

The next chapter presented an overview of the current ray tracing based propagation prediction algorithms. The different ray tracing algorithms present in the literature were described, and the merits and the demerits of the different algorithms were discussed. The computational complexity of a ray tracing based prediction technique was calculated and the limitations of a ray tracing based approach were elaborated.

The standard ray tracing based prediction technique is computationally very intensive, especially while predicting the propagation characteristics of multiple receivers. A novel, computationally less intensive, technique to predict the propagation characteristics of multiple receivers was presented in Chapter 6. This technique uses a variant of standard ray tracing technique, called tube tracing, to predict the signal characteristics of a grid of receivers at a certain elevation above the ground. The new method was verified against the ray tracing method and was found to produce almost identical results. The new method was found to decrease the computation time of a propagation prediction algorithm manifold, especially when the number of receiver points increases.

7.2 Future Work

With the advent of new wireless standards such as Blue-Tooth and W-CDMA, a proliferation of wireless devices is expected in the next few years. More sophisticated wireless system planning tools and accurate propagation prediction mechanisms would be required to make the promise of ‘seamless computing and communication’ a reality. Ray tracing seems to be an obvious choice for propagation prediction. However, the computation time involved, while tracing the rays remains the main stumbling block for a

ray tracing based approach. Parallel processing techniques can be used to greatly reduce this. This is a fresh area of research and holds much promise.

There is a great deal of work still requires in order to produce feasible and accurate ray tracing tool for commercial use. Extensive testing of the proposed grid based ray tracing algorithm is required before it can be used for commercial purposes. For a ray tracing method to be accurate, the dielectric properties of the building materials need to be obtained. Building and terrain information with better resolution is required to improve the accuracy of the ray tracer. The optimum number of reflections and diffraction required to obtain a realistic model of the channel need to be estimated. The ray tracing techniques have to be thoroughly verified with the measured results in terms of the power delay profile and the angle of arrival information, and the margin of error for a ray tracing based prediction technique has to be established.

Appendix A

Appendix A is intended to serve as a quick reference for the programs used to model the terrain and the buildings. All the programs are written in C++ using Micro Soft Visual C++ ver. 6. The reference page provides a brief description of the classes, the functions, the arguments used to call the functions and the Microsoft Foundation Classes (MFC) classes used in the program.

Modeling the Terrain

The program to model the terrain using the Delunay based algorithm is described.

Project Workspace: Delunayterrain.dsw

Project Settings: Use MFC in a static library.

Program arguments: Bald Earth DEM (in an ASCII format).

Header Files:

1) const.h – Defines all the functions used in the project. The maximum size of the DEM need to be specified here.
2) Triangles.h – Defines a class called traingles.
3) Vec3D.h – Defines a vector class.
4) linecount.h – Defines a class called linecount which helps in counting the lines of the polygon while adding a new point to the Delaunay triangulation algorithm. See chapter 4 for details.

Source files:

1) mainprog.cpp – This file implements the main function of the program. The function opens the DEM file and reads the DEM into an array. The function calls the function inittriangulate() and the function Delaunay().

2) Triangles.cpp – All the functions of the class triangle are described in this file.

3) Delaunay.cpp – This file describes the function Delaunay(), which implements the Delaunay triangulation algorithm.
4) Utilities.cpp – This file includes the function body of several utility functions use for finding the 3-D distance between two points and 2-D distance between two points, the square of a number and find the line segment equation given the two end points of the line segment.
5) Check.cpp- This program is used to check if all the points in the DEM are included in the TIN.

General Description:

An array of triangles called '*trarray*' is used as a global variable and stores all the triangles of the TIN representation. A MFC function called *CArray* is used as the base type. The main program reads the input from the program arguments. The main function calls a function *inittriangulate()*, which uses the DEM data and creates two triangles along the diagonal. These two triangles are stored in the global variable *trarray*. The main function then calls the function *Delaunay()*. This function creates the Delaunay triangulates till all the point in the TIN is below a user defined maximum error. The function stores all the triangles in the variable *trarray*. The *trarray* can either be inputted into a file or can be used directly in the propagation prediction program.

Modeling the building

The program used to model the buildings is described here.

Project Workspace: buildsurface.dsw

Project settings: Using MFC in a static library.

Program arguments:

1) foot.dbf – provides with a list of the building footprint elevation along with its buidling number,
2) top.dbf - The ceiling number and the corresponding ceiling elevations are given.

3) Top.gen – The building rooftops are modeled as polygons and the vertices of the polygons are stored along with its ceiling number.

Header Files:

1) genparser.h – defines the constants.

Source Files:

1) roofparse.cpp – Reads the top.gen and parses the file to find the topprint information.
2) Genparser.cpp – Includes the main function and calls the functions parseroof(), createsurface( ) and createlid( ) respectively.
3) Getfootelev.cpp – Parses the elevation of the footprint from foot.dbf.
4) Getroofelev.cpp - Reads the elevation of the rooftop from top.dbf.
5) CreateSurface.cpp - Creates the vertical surface after the information regarding the rooftop elevation and the rooftop shape is acquired.

General Description:

The information regarding the shape of the rooftop is obtained from the file top.gen. The vertices of the different rooftop polygons are stored into a collection class called ‘roofmap’. It uses an MFC class called CMap. The ceiling numbers are used to index the various ceiling polygons. The rooftop elevations are then obtained from top.dbf. The base elevations are obtained from foot.dbf. The function create surface () is called and it constructs vertical polygonal surfaces for the building walls. The ceilings of the buildings are then modeled.

Appendix B

Free space Propagation Model

The free space power received by a receiver antenna, which is separated from a radiating transmitter antenna by a distance d, is given by

$P_r(d) = \frac{P_t G_t G_r l^2}{(4p)^2 d^2 L}$, where P_t is the transmitted power, $P_r(d)$ is the received power, which is a function of T-R separation, G_t is the transmitter antenna gain, G_r is the receiver antenna gain, d is the T-R separation in meters, L is the system loss factor not related to propagation and l is the wavelength in meters.

The gain of the antenna is related its effective aperture, A_e, by

$G = \frac{4p A_e}{l^2}$, The effective aperture A_e is related to the physical size of the antenna, and l is related to the carrier frequency by $l = \frac{c}{f}$, where f is the frequency in Hertz and c is the speed of light given in meters/sec.

Bibliography

1) M. Zeng, A. Annamalai, V.K. Bhargava, "Recent advances in cellular wireless communications," *IEEE Communications Magazine*, vol. 37, Sept. 1999, pp. 128-138.

2) W.Y.C. Lee, "Elements of Cellular Mobile Radio Systems," *IEEE Transactions on Vehicular Technology*, vol. 35, no. 2, May 1986.

3) T.S. Rappaport, *Wireless Communications: Principles and Practice*, Prentice-Hall Inc., New Jersey, 1996.

4) M. Wittmann, J. Marti, T. Kurner, "Impact of the power delay profile shape on the bit error rate in mobile radio systems," *IEEE Transactions on Vehicular Technology*, vol. 46, May 1997, pp. 329-339.

5) H. L. Bertoni, *Radio Propagation for Modern Wireless Systems* , Prentice Hall, New Jersey, 2000.

6) E.K. Tameh, A.R. Nix, M.A.Beach, "A 3-D integrated macro and microcellular propagation model, based on the use of photogrammetric terrain and building data," *IEEE Vehicular Technology Conference*, Vol. 3, 1997, pp. 1957 -1961

7) K. Rizk, J.-F. Wagen, F. Gardiol, "Two-dimensional ray-tracing modeling for propagation prediction in microcellular environments," *IEEE Vehicular Technology Conference*, vol. 46, May 1997, pp. 508 –518

8) W.C.Y.Lee, D.J.Y. Lee, "Microcell prediction by street and terrain data," *IEEE Vehicular Technology Conference*, vol. 3, 2000, pp. 2167 –2171

9) T. Huschka, "Ray Tracing models for Indoor environments and their computational complexity," *Personal, Indoor and Mobile Radio Communications*, 1994, vol. 2, pp. 486-490.

10) A.H. Robinson, J.L. Morrison, P.C. Muehrcke, A.J. Kimberling, S.C. Guptill, *Elements of Cartography,* John Wiley & Sons, New York, 1995.

11) T.S. Rappaport, et. al., "Use of Topographic Maps with Building Information to determine Antenna placement for Radio Detection and Tracking in Urban Environments," *MPRG Technical Report MPRG-TR-96-19*, Dept Of Electrical Engineering, Virginia Polytechnic Institute and State University, Jun 31, 1996.

12) http://www.i3.com

13) http://www.edx.com

14) http://www.usgs.gov

15) D. Larsen. Philip Notestine, " MSFRM – A prediction tool for Radio System design," *IEEE Vehicular Technology Conference*, 1990, pp.- 378-383.

16) R. Lewenz, F. Riddoch, D. King, "Enhanced UHF propagation predictions in rural areas using a high resolution clutter database," *IEEE International Conference on Antennas and Propagation*, vol. 2, 1997 , pp. 210 –213.

17) G. Lampard, T. Vu-Dinh, "The effect of terrain on radio propagation in urban microcells," *IEEE Transactions on Vehicular Technology*, vol. 42, Aug. 1993, pp. 314-317.

18) Y. Okumura, E. Ohmori, T. Kawano, and K. Fakuda, "Field Strength and Its variability in VHF and UHF Land-Mobile Radio Service," *Rec. Elec. Commun. Lab.*, vol. 16, pp. 825-873, 1968.

19) W.C.Y. Lee, "Studies of base station antenna height effects on mobile radio," *IEEE Transactions on Vehicular Technology*, vol. VT 29, May 1980, pp. 252-260

20) L. Piazzi, H.L. Bertoni, "Effect of terrain on path loss in urban environments for wireless applications," *IEEE Transactions on Antennas and Propagation*, vol. 46, Aug. 1998, pp: 1138 –1147

21) J.D. Parsons, *The Mobile Radio Propagation Channel*, 1st ed. Wiley ,New York, 1992.

22) G. Stratis, J. Mendoza, A. Veeraraghavan, "Method and apparatus for predicting signal characteristics in a wireless communication system," U.S. Patent No-5,953,669, Sept.14, 1999

23) C.S. Rajguru, "Applications of GIS in propagation prediction," Master's Thesis in Electrical Engineering, Virginia Polytechnic Institute and State University, Blacksburg VA., Aug. 22, 1992

24) J. Lee, "Assessing the existing methods for TIN extraction," AUTO-CARTO 10, *Proceedings Of International Symposium On Computer-Assisted cartography*, ACSM-ASPRS, vol. 2, 1991, pp. 194-203

25) R.J. Fowler, and J.J. Little, "Automatic Extraction of Irregular Network Digital Terrain Models," *ACM*, 1979 vol. 4, pp.199-200.

26) Z. Chen and J A Guevara, “Systematic Selection of Very Important Points Algorithm from Digital Terrain Model for constructing Triangular Irregular Networks,” *Auto Carto 8*, 1987, pp. 50-60.

27) L. DeFloriani, B. Falcedieno, C. Nagy, C. Pienovi, “A hierarchical Structure for surface Approximation,” *Computers and Graphics*, 1984, vol. 8(2), pp. 183-193.

28) http://www.esri.com/software/arcinfo/

29) http://www.ncgia.ucsb.edu/giscc/units/u056/u056.html

30) A. Mirante, N. Weingarten, “Radial Sweep Algorithm for constructing Triangular Irregular Network,” *IEEE Computer Graphics and Applications*, vol. 2, May 1982, pp. 11-21.

31) D. Salomon, ”Computer Graphics & Geometric Modeling,” Springer, NY, 1996

32) B.A. Lewis , J.S. Robinson, “Triangulation of Planar regions with applications,” *The Computer Journal*, 1978, vol 21, no 4, pp. 324- 332.

33) M.F. Polis, D.M. McKeown, Jr., “Iterative TIN generation from digital evaluation models,” *Proceedings CVPR* '92.,1992, pp. 787 – 790.

34) G.E. Athanasiadou, A.R. Nix, J.P. McGeehan, “A ray tracing algorithm for microcellular wideband propagation modelling,” *IEEE Vehicular Technology Conference*, vol.1 , 1995, pp. 261 -265

35) J.P. Rossi, J.C. Bic, A.J. Levy, Y. Gabillett, M. Rosen, “A ray launching method for radio-mobile propagation in urban area,” *Antennas and Propagation Society International Symposium*, 1991. AP-S. Digest , vol. 3, 1991, pp. 1540 -1543

36) B.E. Gschwendtner, F.M. Landstorfer, ”3-D propagation modeling in microcells including terrain effects,” *Personal, Indoor and Mobile Radio Communications*, 1995. PIMRC'95, vol. 2, pp. 532 -536

37) K.R. Schaubach, N.J. Davis, T.S. Rappaport, “A ray tracing method for predicting path loss and delay spread in microcellular environments,” *IEEE Vehicular Technology Conference*, vol. 2, 1992, pp. 932 –935.

38) K. Rizk, J. –F, Wagen, F. Gardiol, “Influence of database accuracy on two-dimensional ray-tracing-based predictions in urban microcells,” *IEEE Transactions on Vehicular Technology*, vol. 49, March 2000, pp. 631 –642.

39) T. Kurner, D.J. Cichon ,W. Wiseback, “Concepts and results for 3-D Digital terrain – based wave propagation models: An overview,” *IEEE Journal on Selected Areas in communication*, vol. 11, Sept. 1993, no 7, pp. 1002-1012.

40) G.E. Athanasiadou, A.R. Nix, “Investigation into the sensitivity of the power predictions of a microcellular ray tracing propagation model,” *IEEE Transactions on Vehicular Technology*, vol. 49, July 2000, pp. 1140 –1151.

41) M. Hata, “Emperical Formula for Propagation Loss in Land Mobile Radio Service,” *IEEE Transactions on Vehicular Technology*, vol. VT-29, 1980, pp.317-325.

42) F. Ikegami, S. Yoshida, T. Takeuchi, and M. Umehira, “ Propagation Factors Controlling Mean Field Strength on Urban Streets,” *IEEE Transactions on Antennas and Propagation*, vol. AP-32, pp. 822-829, 1980

43) J. Walfish , H.L. Bertoni, “A theoretical Model of UHF Propagation in Urban Environments,” *IEEE Transactions on Antennas and Propagation*, vol. AP-36, pp. 1788-1796, 1988.

44) H.L. Bertoni, W. Honcharenko, L.R. Maciel, H.H. Xia, “UHF Propagation Prediction for Wireless Personal Communications,” *Proceedings of IEEE*, vol. 82, pp. 1333-1359, 1994.

45) J. McKown, R.L. Hamilton, “Ray tracing as a design tool for radio networks,” *IEEE Network Magazine*, vol. 5, No. 6, pp. 27-30, Nov 1991.

46) R.A. Valenzuela,”Ray tracing prediction of indoor radio propagation,” *IEEE PIMRC*, vo1. 1, pp. 140-144, 1994.

47) Seong-Cheol Kim, B.J. Guarino Jr, T.M. Willis III, V. Erceg, S.J. Fortune, R.A. Valenzuela, L.W. Thomas, J. Ling, J.D. Moore, “Radio propagation measurements and prediction using three-dimensional ray tracing in urban environments at 908 MHz and 1.9 GHz ,” *IEEE Transactions on Vehicular Technology*, vol. 48, May 1999, pp. 931 –946.

48) M.C. Lawton, J.P. McGeehan, “The application of a deterministic ray launching algorithm for the prediction of radio channel characteristics in small-cell environments,” *IEEE Transactions on Vehicular Technology*, vol. 43, Nov 1994, pp. 955-969.

49) S.Y. Seidel, T.S. Rappaport, “Site-specific propagation prediction for wireless in-building personal communication system design,” *IEEE Transactions on Vehicular Technology*, vol. 43, Nov. 1994, pp. 879-891.

50) S.Y. Tan, H.S. Tan, “Propagation model for Microcellular Communications Applied to Path Loss Measurements in Ottawa City Streets,” *IEEE Transactions on Vehicular Technology*, vol. 44, pp. 313-317, 1995.

51) H.H. Xia, A.B. Herrera, S. Kim, F.S. Rico, "A CDMA-distributed antenna system for in-building personal communications services," *IEEE JSAC*, vol. 14, May 1996, pp. 644-650.

52) C. A. Balanis, *Advanced Engineering Electromagnetics*, John Wiley & Sons, New York, 1989

53) J.B. Keller, "Geometrical Theory of Diffraction," *Journal of the Optical Society of America*, vol. 52, no. 2, pp. 116-130, Feb. 1962.

54) R.F. Kouyoumjian, P.H. Pathak, "A Uniform Theory of Diffraction for an Edge in a perfectly conducting Surface," *IEEE Proceedings*, Vol. 62, pp. 1448-1461, 1974.

55) W. Honcharenko, H.L. Bertoni, "Prediction of wideband RF propagation characteristics in buildings using 2D ray tracing," *IEEE Vehicular Technology Conference*, vol. 1, 1995, pp. 429-433.

56) W. K. Tam, V.N. Tran, "Multi-Ray Propagation Model for Indoor Wireless Communications," *IEE Electronics Letters*, vol. 32, no.2, pp. 135-137, Jan 1996.

57) A. Falsafi, K. Pahlavan, G. Yang, "Transmission techniques for radio LAN's-a comparative performance evaluation using ray tracing", *IEEE JSAC*, vol. 14, April 1996, pp. 477-491.

58) H.Meng, P. Koushik, T.S. Rappaport, "Comparitive study of indoor and outdoor site-specific propagation prediction models," Tech. Report MPRG-TR-93-07, Virginia Tech, Feb 1993.

59) G. Durgin, N. Patwari, T.S. Rappaport, "An advanced 3D ray launching method for wireless propagation prediction," *IEEE Vehicular Technology Conference*, vol. 2, 1997, pp. 785-789.

60) G. Durgin, *Advanced Site Specific Propagation prediction techniques*, Master's Thesis in Electrical Engineering, Virginia Polytechnic Institute and State University, Blacksburg VA., May 1998.

61) D.J. Cichon, T. Zwick, J. Lahteenmaki, "Ray optical indoor modeling in multi-floored buildings: simulations and measurements," *IEE Antennas and Propagation Society International Symposium*, 1995 Digest , vol. 1 , 1995 , pp. 522-525.

62) P. Kreuzgruber, P. Unterberger, R. Gahleitner, "A ray splitting model for indoor radio propagation associated with complex geometries," *IEEE Vehicular Technology Conference*, 1993, pp. 227-230.

63) P.S. Heckbert, P. Hanarahan, "Beam Tracing Polygonal Objects," *Computer Graphics*, 18(3), pp. 119-127, July 1984.

64) S. Fortune, “Efficient algorithms for prediction of indoor radio propagation,” *IEEE Vehicular Technology Conference*, 1998, vol. 1, pp. 572-576.

65) G. Liang, H.L. Bertoni, “A new approach to 3-D ray tracing for propagation prediction in cities,” *IEEE Transactions on Antennas and Propagation*, Vol. 46, June 1998, pp. 853-863.

66) A .S. Glassner, *An Introduction to Ray Tracing*, Academic Press, San Diego, 1989.

67) H.D. Sherali, C.M. Pendyala, T.S. Rappaport, “Optimal location of transmitters for micro-cellular radio communication system design,” *IEEE JSAC*, vol. 14, May 1996, pp. 662-673.

68) H.H. Xia, A.B. Herrera, S. Kim, F.S. Rico, “A CDMA-distributed antenna system for in-building personal communications services,” *IEEE JSAC*, vol. 14, May 1996, pp. 644-650.

69) A. Molina, A.R. Nix, G.E. Athanasiadou, “Cellular network capacity planning using the combination algorithm for total optimization,” *IEEE Vehicular Technology Proceedings*, VTC-2000, vol. 3, pp. 2512-2516.

70) W. M. O'Brien, E. M. Kenny, P.J. Cullen, “An efficient implementation of a three-dimensional microcell propagation tool for indoor and outdoor urban environments,” *IEEE Transactions on Vehicular Technology*, vol. 49, March 2000, pp. 622-630.